Biomedicine & Pharmacotherapy 174 (2024) 116514

Contents lists available at ScienceDirect

Biomedicine & Pharmacotherapy

journal homepage: www.elsevier.com/locate/biopha

# Industrial-produced lemon nanovesicles ameliorate experimental colitis-associated damages in rats via the activation of anti-inflammatory and antioxidant responses and microbiota modification

Vincenza Tinnirello [a,1], Maria Grazia Zizzo [b,1], Alice Conigliaro [a], Mariangela Tabone [c,d], Nima Rabienezhad Ganji [a], Adele Cicio [b], Carlo Bressa [c,e], Mar Larrosa [c,f], Francesca Rappa [g,h], Giuseppe Vergilio [g], Roberta Gasparro [a], Alessia Gallo [i], Rosa Maria Serio [b], Riccardo Alessandro [a,j,2], Stefania Raimondo [a,2,*]

[a] Department of Biomedicine, Neurosciences and Advanced Diagnostics (Bi.N.D), University of Palermo, Section of Biology and Genetics, Palermo 90133, Italy
[b] Department of Biological, Chemical and Pharmaceutical Sciences and Technologies (STEBICEF), University of Palermo, Viale delle Scienze, Palermo 90128, Italy
[c] MAS Microbiota Group, Faculty of Biomedical and Health Sciences, Universidad Europea de Madrid, Madrid 28670, Spain
[d] Faculty of Biomedical and Health Sciences, Universidad Europea de Madrid, Madrid 28670, Spain
[e] Faculty of Experimental Sciences, Universidad Francisco de Vitoria, Madrid 28670, Spain
[f] Department of Nutrition and Food Science, School of Pharmacy, Complutense University of Madrid, Madrid, Spain
[g] Department of Biomedicine, Neurosciences and Advanced Diagnostics (BIND), Institute of Human Anatomy and Histology, University of Palermo, Palermo 90127 Italy
[h] Institute of Translational Pharmacology, Section of Palermo, National Research Council (CNR), Palermo 90146, Italy
[i] Research Department, IRCCS-ISMETT (Istituto Mediterraneo per i Trapianti e Terapie ad Alta Specializzazione), Palermo 90127, Italy
[j] Institute for Biomedical Research and Innovation (IRIB), National Research Council (CNR), Palermo 90146, Italy

ARTICLE INFO

*Keywords:*
Plant-derived nanovesicles
*Citrus limon* L.
Inflammatory bowel disease
Inflammation
Oxidative stress
Microbiota

ABSTRACT

Plant-derived nanovesicles (PDNVs) have recently emerged as natural delivery systems of biofunctional compounds toward mammalian cells. Considering their already described composition, anti-inflammatory properties, stability, and low toxicity, PDNVs offer a promising path for developing new preventive strategies for several inflammatory diseases, among which the inflammatory bowel disease (IBD). In this study, we explore the protective effects of industrially produced lemon vesicles (iLNVs) in a rat model of IBD. Characterization of iLNVs reveals the presence of small particles less than 200 nm in size and a profile of bioactive compounds enriched in flavonoids and organic acids with known beneficial properties. *In vitro* studies on human macrophages confirm the safety and anti-inflammatory effects of iLNVs, as evidenced by the reduced expression of pro-inflammatory cytokines and increased levels of anti-inflammatory markers. As evidenced by *in vivo* experiments, pre-treatment with iLNVs significantly alleviates symptoms and histological features in 2,4 dinitrobenzensulfuric acid (DNBS)-induced colitis in rats. Molecular pathway analysis reveals modulation of NF-κB and Nrf2, indicating anti-inflammatory and antioxidant effects. Finally, iLNVs affects gut microbiota composition, improving the consistent colitis-related alterations. Overall, we demonstrated the protective role of industrially produced lemon nanovesicles against colitis and emphasized their potential in managing IBD through multifaceted mechanisms.

## 1. Introduction

Inflammatory Bowel Disease (IBD) is a class of chronic relapsing inflammatory disorders [1], including Crohn's disease (CD) and ulcerative colitis (UC), with unknown aetiology. The causes of IBD onset are multifactorial, attributable to the interplay of genetic, environmental, microbial, and immunologic factors. It has been hypothesized that in a genetically predisposed individual, an inappropriate and persistent inflammatory response is established against the commensal bacterial community, resulting in chronic inflammation and damage to the gut

* Corresponding author.
*E-mail address:* stefania.raimondo@unipa.it (S. Raimondo).
[1] These authors contributed equally
[2] Last authors

https://doi.org/10.1016/j.biopha.2024.116514
Received 30 January 2024; Received in revised form 13 March 2024; Accepted 28 March 2024
Available online 3 April 2024

[2–4]). One of the main consequences of chronic inflammation, as well as the peculiarities of such diseases, is the alteration of intestinal permeability, physiologically maintained by tight junctions. In IBDs, a cascade of events emerges in which the changed permeability permits antigens and microorganisms, including commensal ones, to penetrate the lamina propria, to activate immune system cells, triggering the release of inflammatory mediators, which exacerbates the phlogistic condition [5]. In a complex scenario where multiple causes cooperate to determine the occurrence of the disorder, reactive oxygen species (ROS), produced by the cells of the immune system, are involved, driving the inflammatory process and promoting the pathogenesis of IBD. Typically, endogenous antioxidants can efficiently mitigate oxidative stress in the intestinal mucosa. However, in the case of IBD, inflammation leads to an imbalance between pro-oxidants and antioxidants due to the increased requirement for the latter, resulting in mucosal damage [6–9]. Currently, there is no curative treatment, and therapeutic strategies mainly aim to alleviate symptoms. Conventional therapy involves the use of anti-inflammatory agents such as corticosteroids, 5-aminosalicylates, and immunosuppressants which usually provide significant suppression of inflammation and relief of symptoms [10–12]. However, a significant portion of patients do not respond to treatment or became resistant during the time; moreover, long-term therapies often result in adverse effects. For these reasons, the need for new preventive and curative approaches is urgent [8,13–15]. In recent years, alongside common drugs, increasing attention has been paid to substances of natural origin. Promising *in vitro* and *in vivo* studies have shown that they are an excellent source of compounds with therapeutic, antioxidant, and anti-inflammatory properties, potentially useful for the management and prevention of IBD [16–20]. Phytochemicals, including phenolics and polyphenols, naturally occurring in plants, fruits, and vegetables, can exert preventive and therapeutic effects through down-regulation of inflammatory cytokines and enzymes and by the enhancement of antioxidant defense [21–23]. Among the substances derived from the plant kingdom, a crucial but less explored role, in the field of IBD, could be attributed to plant-derived nanovesicles (PDNVs), nano-sized lipid-bilayer vesicles produced by several plant species that have increasingly fascinated the scientific community. Although their role in nature is related to plant immune response, plant-derived nanovesicles can interact with mammalian cells, mediating cross-kingdom communication. Increasing evidence shows that PDNVs exert anti-tumor properties [24–26], reduce oxidative stress [27,28], modulate the gut microbiota [29,30], and reduce inflammation in several *in vitro* and *in vivo* models [31,32]. In addition, their high stability and ability to overcome biological barriers, combined with the possibility of large-scale and low-cost production, make them attractive for preventive purposes [33,34]. Several research groups have already characterized the protein, lipid, RNA, and metabolite content of nanovesicles isolated from many plant matrices, such as ginger [35,36], grapefruit [37], grape [38], blueberry [39] and broccoli [40]. Our research group has previously isolated and characterized nanovesicles from Citrus limon (LNVs) [25,28,41], demonstrating their anti-inflammatory and antioxidant properties *in vitro* and *in vivo*. In particular, we found that LNVs exert anti-inflammatory effects on murine and human immune system cells through the inhibition of NF-kB/ERK1–2 pathways [41] as well as in zebrafish embryos [28].

To the best of our knowledge, although the biological properties of nanovesicles purified from lemon have been highlighted in several studies [25,28,41], there is no data on their impact on IBD. This work aims to investigate the anti-inflammatory activity of industrially produced lemon nanovesicles (iLNVs) and their potential utility in the preventive treatment of IBD. To achieve this, we first characterize and analyze the contents of iLNVs, their anti-inflammatory activity in macrophages, and we studied *in vivo* the effects on an experimental model of IBD, the 2,4-dinitrobenzene sulfonic acid (DNBS)-induced colitis in rat.

## 2. Materials and methods

### 2.1. Isolation of nanovesicles from Citrus limon at industrial scale (iLNVs)

Nanovesicles were isolated at an industrial scale (iLNVs) using a patented process (IT patent n° 102019000005090, International Application No.PCT/IB2020/053183: “Process for the production of vesicles from citrus juice”, https://pantentscope.wipo.int/search/en/detail.jsf?docId=W2020202086). Briefly, lemon juice was obtained at Agrumaria Corleone s.p.a. (Palermo, Italy), centrifuged at 5000 rpm for 55 seconds, and ultrafiltered using semi-porous membranes with pore size 50,000 Dalton. The retentate of the ultrafiltered juice was further purified by microfiltration with a cut-off of 0.45 μm until a permeate-containing vesicles was obtained.

### 2.2. Nanoparticle tracking analysis

Nanoparticle Tracking Analysis (NTA) was carried out to measure the size distribution and concentration of iLNVs (NanoSight NS300, Malvern Instruments Ltd, UK) as previously described [42]. Samples were diluted 1:100 in PBS to reach an optimal concentration to maintain the linearity of the instrument. Particle size measurement was calculated in three 60-s videos on a particle-by-particle basis to supply accurate statistics for each analysis. Measurements were conducted under the following conditions: cell temperature: 23.5°-23.6°C; syringe velocity: 30 μl/s. The registered data were analyzed for mean, mode, median, and estimated particle concentration by NanoSight NTA 3.3 software with a detection threshold of 5. Hardware: built-in laser: 45 mW at 488 nm; camera: sCMOS.

### 2.3. Qualitative and quantitative metabolomic characterization

Qualitative and quantitative characterization of iLNV metabolites was carried out at the Botanicals Lab of the Fondazione Toscana Life Sciences (Siena, Italy). Qualitative analysis of iLNVs was performed by UHPLC-UV-ESI-MS. Q-Exactive Plus mass spectrometer (ThermoFisher Scientific) equipped with an electrospray source (ESI) and coupled to an Ultimate 3000 SD UHPLC (ThermoFisher Scientific). The injected samples were separated using a Waters BEH C18 Acquity UPLC column (2.1 mm×15 cm, 1.7 μm, Waters). Separation with eluent A (H2O + 0.1% (v/v) formic acid) and eluent B (acetonitrile + 0.1%(v/v) formic acid) was performed in a 50-min gradient at a flow rate of 0.2 mL/min. Quantitative analysis was performed with different instrumentation depending on the compounds investigated.

*Flavonoids* were quantified by HPLC-ESI-MS/MS using a TSQ Quantum Access mass spectrometer (ThermoFisher Scientific) equipped with an electrospray source (ESI) and coupled to an Agilent 1100 Liquid Chromatograph (Agilent). Quantitative analysis was performed using single reaction monitoring (SRM) experiments. Gradient: eluent phases 0.1% formic acid in H2O (phase A) and 0.1% formic acid in acetonitrile (phase B). The analysis was conducted in gradient with initial condition 10% phase B for 1 minute, subsequent increase to 20% in 12 minutes, and further increase to 100% in the next 5 minutes. Sample volume: 20 μl Chromatographic column: XBridgeTM C18 3.5μm 2.1 mm x 100 mm (Waters). The analyses were performed in a positive mode. hesperidin, luteolin-7-rutinoside, and eriocitrin were quantified using SRM experiments, which are based on the identification of characteristic fragmentations for each compound. In detail, for eriocitrin, the protonated species [M+H]+ at *m/z* 597 with respective fragments at *m/z* 435 and 289 was selected; for hesperidin, the protonated species [M+H]+ at *m/z* 611 with respective fragments at *m/z* 449 and 303; and for luteolin-rutinoside, the protonated species [M+H]+ at *m/z* 595 with respective fragments at *m/z* 449 and 287.

*Citric acid and isocitric acid* content were quantified by UHPLC-UV-ESI-MS consisting of a Q-Exactive Plus mass spectrometer

(ThermoFisher Scientific) equipped with an electrospray source (ESI) and coupled to an Ultimate 3000 SD UHPLC (ThermoFisher Scientific). Analyses were conducted in negative ESI mode. Gradient: eluent phases 0.1% formic acid in H2O (phase A) and 0.1% formic acid in acetonitrile (phase B). The analysis was conducted in a 5-min gradient, with initial and final conditions of 60% B and 10% B, respectively. Chromatographic column: Acquity UPLC Waters BEH HILIC (1.0 mm×10 cm, 1.7 µm, Waters). Flow rate: 0.1 mL/min Sample volume: 10 µl. For Citric and Isocitric acid, it was necessary to rely on the fragmentation study to identify "unique" fragmentations for each. Analyses were conducted in a negative mode in this case, and the following characteristic fragmentations were considered: for citric acid, the protonated species [M-H]- at *m/z* 191 was selected with the respective fragment at *m/z* 111, while for isocitric acid, the deprotonated species (M-H]- at *m/z* 191) was selected with the fragment at *m/z* 155.

For each analyte, solutions of increasing known concentration were analyzed to obtain the calibration curves for each, checking their linear trend over the chosen concentration range, and finally the samples. On these, the areas obtained for the same analytes in the analyzed samples were interpolated.

### 2.4. Scanning electron microscope (SEM)

Electron microscopy images were acquired by a FEI-ThermoFisher Versa 3D electron microscope, operating at 10 kV at a working distance of 9.3–10.3 mm. The sample was deposited on a 3 mm copper holey carbon coated grid (TAAB); the solvent was evaporated at room temperature overnight.

The grids were mounted on a STEM sample holder and the samples were analyzed with 2 different techniques simultaneously: morphological analysis was performed through secondary electron (SE), while the structural details of the samples were evaluated by transmitted electron (TE). Micrographs were acquired at different magnifications, from 5000x up to 70000x.

### 2.5. Cell culture

The human monocyte THP-1 cell line was obtained from ATCC (Manassas, VA, USA). Cells were cultures in RPMI-1640 medium (ATCC, Manassas, VA, USA) supplemented with 10% FBS, 100 U/mL penicillin, and 100 µg/mL streptomycin (Euroclone, UK). THP-1 monocytes were differentiated into M0 macrophages (THP-1 M0) according to the manufacturer's instructions and as described in the literature [43]. Specifically, cells were plated at 1 $\times 10^5$ cells/mL and incubated at 37°C with 5% $CO_2$ for 48 hours in the presence of 50 ng/mL of Phorbol 12-myristate 13-acetate (PMA, Sigma-Aldrich, Saint Luis, MO, USA); subsequently, the medium was discarded and replaced with fresh medium for 3 days for cell recovery. The cells were then treated with different doses of iLNVs as described below.

### 2.6. Cell viability assays

Cell viability of the THP1 M0 cells was determined by MTT (3-[4,5-Dimethylthiazol-2-yl]-2,5 Diphenyl Tetrazolium Bromide) assay as previously described [44]. Human monocytes, THP-1 cell line, were seeded in triplicate at 2 $\times 10^4$ cells/well in 48-well plates and induced to differentiate into macrophages (THP-1 M0) as previously described [44]. THP-1 M0 was treated for 24 and 48 hours with two different doses (2,5 and 5 µg/mL) of iLNVs; these doses were selected in accordance with our previous studies [25,41]. At the treatment endpoint, MTT was added for 3 hours and cells were then lysed with isopropanol. The absorbance was measured by an ELISA reader at 540 nm (Microplate Reader, BioTek, Winooski, VT, USA). Values are expressed as a percentage of cell growth versus control (untreated cells).

### 2.7. Animals

Twenty Wistar male rats (weighing 200–300 g), were purchased from ENVIGO Srl (San Pietro al Natisone UD, Italy) and employed throughout the study. The animals were housed in temperature-controlled rooms on a 12 h light cycle at 22–24°C and 50–60% humidity. They were fed standard laboratory chow and tap water ad libitum. The animals were allowed to acclimatize to the housing conditions for 1 week before experimentation. Procedures involving the animals and their care were conducted in conformity with the Italian D.Lgs 26/2014" and the European directives (2010/63/EU). The experiments had been approved by the Ethical Committee for Animal Experimentation of the University of Palermo and by the Italian Ministry of Health (Authorization n 921/2018–released Rome, Italy). No other methods to perform the described experiments (3Rs) were found.

### 2.8. DNBS-colitis induction and treatment protocol

Five hundred microliters of iLNVs, corresponding to 0.6 mg/kg, were administered by oral gavage once a day for 14 days starting 7 days before the induction of colitis (day −7). Rats were randomly assigned to 4 groups (5 animals each): 1) sham group; 2) iLNVs (0.6 mg/Kg/day); 3) DNBS (colitis group); 4) iLNVs (0.6 mg/Kg/day) +DNBS. Colitis was induced by intracolonic (i.c.) instillation of DNBS, as already described [45]. Briefly, rats were fasted overnight and then, under light anesthesia with 1% isoflurane (Merial Italia Spa, Assago, MI, Italy), a solution of 25 mg of 2, 4-dinitrobenzene sulfonic acid (DNBS; Sigma-Aldrich Inc., St Louis, MO, USA) in 50% ethanol, total volume of 0.25 mL, was injected into the colon through an 8 cm plastic catheter (PE90). Rats were then maintained in an inclined position for 3 min and allowed to recover with food and water supplied. Sham animals received 0.25 mL of the vehicle alone (50% ethanol). Previous experiments demonstrated that 25 mg DNBS induced reproducible colonic inflammation manifested by the clinical signs as well as macroscopic damage and biochemical alterations characteristic of the disease. No mortality was observed in any group throughout the study. The severity of colitis was evaluated by independent observers blinded to the identity of the treatments, following the criteria previously reported by Zizzo et al. [45] and efforts were made to minimize the suffering of animals.

The experimental plan of *in vivo* study is shown in Fig. 1.

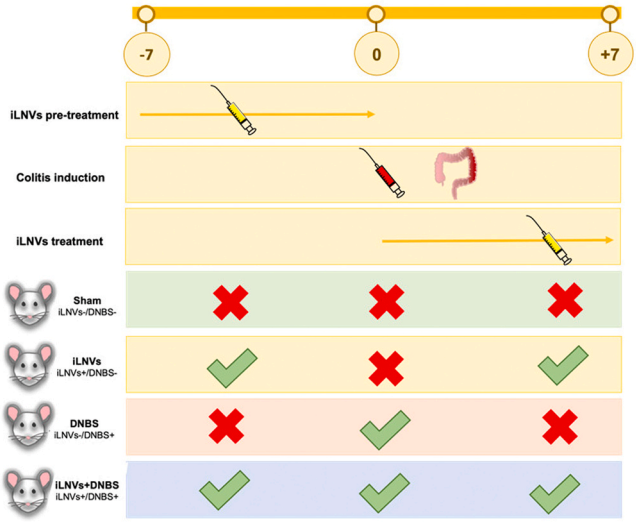


**Fig. 1. :** Schematic representation showing colitis model establishment in rats and treatment design.

### 2.9. Assessment of colitis damage

Body weight, stool consistency, and the presence of blood in the stools were recorded daily for each rat, and the data was used to calculate the disease activity index (DAI) as described by Kullmann et al. [46]. The score ranged between 0–4 for all three parameters and was composed as follows: 1) weight loss (Percent of weight loss at the end of the experiment relative to the first day was calculated for all the groups): none = 0, 1–5% = 1, 5–10% = 2, 10–20% = 3, >20% = 4. 2) Stool consistency: normal pellets = 0, loose stools which do not stick to the anus = 2, diarrhea = 4. 3) Bleeding: none = 0, hemoccult = 2, gross bleeding = 4. After sacrifice the length of the colon segment from the cecum to the rectum was measured. For each specimen wet weight (mg) and length (cm) were measured and the weight/length ratio was calculated as an indicator of colonic edema. The distal part of the rat colon was removed, opened, and rinsed with ice-cold saline solution. Colon sections were blotted dry, weighed, and examined for ulcerated and inflamed regions. The number of ulcers was counted and scored, their area was measured, and colon sections were frozen in liquid nitrogen and stored at −80°C. A total macroscopic damage score was calculated for each animal according to the criteria described by Appleyard and Wallace [47], as outlined in Table 1.

### 2.10. RNA isolation, cDNA synthesis and Real-time PCR

Human monocytes, THP-1 cell line, were plated at 1 $\times 10^5$ cells per mL in 12-well plates and induced to differentiate into macrophages (THP-1 M0) as previously described [44]. THP-1 M0 cells were treated with 5 μg/mL of iLNVs for 24 h and subsequently exposed to the inflammatory stimulus with 1μg/mL of LPS for 3 h. At the end of the treatment, RNA was isolated using the commercially available Illustra RNA spin Mini Isolation Kit (GE Healthcare, Little Chalfont, Buckinghamshire, UK), according to the manufacturer's instructions. Colon biopsies, kept after explantation at −80°C in RNA later, were dried and treated with liquid nitrogen to crystallize the tissue. Subsequently, the samples were homogenized using a mechanical homogenizer in lysis buffer. Total RNA was extracted following the protocol provided by the Illustra RNA spin Mini Isolation Kit (GE Healthcare, Little Chalfont, Buckinghamshire, UK), and its quantification and quality were determined with the NanoDrop spectrophotometer (NanoDrop Technologies, USA). Total RNA from human THP-1 M0 cells and colon biopsies were reverse transcribed to cDNA using the High-Capacity cDNA Reverse Transcription kit (Applied Biosystems, Foster City, CA, USA).

The cDNA from THP-1 M0 cells and colon biopsies were subjected to real-time polymerase chain reaction (RT-PCR) analysis. The sequences of the primers used are listed in Table 2:

**Table 1**
Criteria for macroscopic scoring system adapted from Appleyard & Wallace [47].

| FEATURE | SCORE |
|---|---|
| **Ulceration** | |
| Normal aspect mucosal | 0 |
| Localized hyperemia with no ulcers | 1 |
| Ulceration without hyperemia/bowel wall thickening | 2 |
| Ulceration with hyperemia/bowel wall thickening at 1 site | 3 |
| Two or more sites of ulceration with hyperemia/bowel wall thickening | 4 |
| Major damage (necrosis) extended > 1 cm along length of colon | 5 |
| When an area of damage extended > 2 cm along length of colon; the score was increased by 1 for each additional cm involved | 6–10 |
| **Adhesion** | |
| No adhesions | 0 |
| Minor adhesions (colon can be separated easily from the other tissue) | 1 |
| Major adhesions | 2 |
| **Thickness** | |
| Maximal bowel wall thickness(x) in mm was added to above score | X |

RT-PCR was performed using Step One Real-time PCR System (Applied Biosystem) in a 20 μl reaction containing 300 nM of each primer, 2 μl template cDNA, 18 μl 2X SYBR Green I Master Mix. The RT-PCR was run at 95 °C for 20 sec followed by 40 cycles of 95 °C for 3 sec and 60 °C for 30 sec. Actin was used as the endogenous control. Relative changes in THP-1 M0 cells gene expression between control and treated samples were determined using the ΔΔCt method. The absolute target gene expression in each sample of colon tissue was expressed as 2^ ΔCt, where ΔCt is (Ct gene of interest - Ct internal control). Actin was used as the internal control gene.

### 2.11. Enzyme-linked immunosorbent assay (ELISA) assay

THP-1 cells were plated at 1 $\times 10^5$ cells per mL in 12-well plates and induced to differentiate into macrophages (THP-1, M0) as previously described [44]. THP-1 M0 cells were treated with 5 μg/mL of iLNVs for 24 h and subsequently exposed to the inflammatory stimulus with 1μg/mL of LPS for 3 h. After that, the cell-conditioned medium was collected and centrifuged to remove floating cells and cellular debris. The amounts of pro-inflammatory cytokines, IL-6, and TNF-α and the anti-inflammatory cytokine IL-10 in the conditioned medium were determined using the TNF-α specific enzyme-linked immunosorbent assay (ELISA) kit (Thermo Fisher Scientific) and the IL-6 and IL-10 specific enzyme-linked immunosorbent assay (ELISA) kits (R&D Systems, Inc. (Minneapolis, MN, USA) according to the manufacturer's instructions.

### 2.12. Myeloperoxidase assay

Myeloperoxidase (MPO) activity, a marker for neutrophil inflammation, was estimated according to the method of Moreels et al. [48]. Briefly, samples were blotted dry, weighted, and homogenized in a potassium phosphate buffer (pH 6.0) containing 0.5% hexadecyl trimethylammonium bromide (5 g tissue per 100 mL buffer). Homogenate was subjected to two sonication and freeze-thawing cycles and the suspension was centrifuged at 15000 g for 15 min at 4°C. On a 96 well-plate, 2.9 mL of o-dianisidine solution (16.7 mg of o-dianisidine in 1 mL methanol, 98 mL 0.05 M potassium phosphate buffer pH 6.0 and 1 mL of a 0.5% $H_2O_2$ solution as a substrate for MPO enzyme) was added to 0.1 mL of the supernatant. The absorbance rate was measured at 460 nm (Beckman-Coulter Inc, CA, USA). MPO activity was expressed as units per gram tissue (U gram tissue$^{-1}$), being one unit defined as the amount of the enzyme converting 1 μmol $H_2O_2$ to $H_2O$ in 1 min at room temperature.

### 2.13. Histomorphological analysis

Colon samples were fixed in formalin and embedded in paraffin. Colon tissue sections with a thickness of 5 μm were obtained from paraffin blocks using the microtome and stained with hematoxylin and eosin (H&E) for histological examinations. Sections on the slides were de-waxed in xylene for 10 min and rehydrated by sequential immersion in decreasing ethanol concentrations. The sections were then stained with H&E and examined using an optical microscope (Microscope Axioscope 5/7 KMAT, Carl Zeiss, Milan, Italy) connected to a digital camera (Microscopy Camera Axiocam 208 color, Carl Zeiss, Milan, Italy) for morphological analysis.

### 2.14. Immunohistochemistry

The immunohistochemical experiments were performed on colon tissue sections, 5 μm thick, obtained from paraffin blocks with a cutting microtome. To deparaffinize the sections, the slides were placed in an oven at 60°C for 30 minutes and then immersed in xylene for 30 min at 60 °C. Subsequently, they were rehydrated by immersions in a decreasing scale of alcohols (alcohol 100° for 10 minutes, 95° for

**Table 2**
Primer sequences used in Real-Time PCR.

| **Human** | | |
|---|---|---|
| **Gene** | **Forward Sequence (5to 3)** | **Reverse Sequence (5to 3)** |
| Actin | TCCCTTGCCATCCTAAAAAGCCACCC | CTGGGCCATTCTTCCTTAGAGAGAAG |
| IL-6 | GGTACATCCTCGACGGCATCT | GTGCCTCTTTGCTGCTTTCAC |
| TNF-α | CCAGGCAGTCAGATCATCTTCTC | AGCTGGTTATCTCT CAGCTCCAC |
| IL-10 | GCTGAGAACCAAGACCCAGA | GCATTCTTCACCTGCTCCAC |
| **Rat** | | |
| **Gene** | **Forward Sequence (5to 3)** | **Reverse Sequence (5to 3)** |
| Actin | AAGGCCAACCGTGAAAAGAT | TGGTACGACCAGAGGCATAC |
| IL-6 | TCTATACCACTTCACAAGTCGGA | GAATTGCCATTGCACAACTCTTT |
| Occludin | CTACTCCTCCAACGGCAAAG | AGTCATCCACGGACAAGGTC |

5 minutes, 70° for 5 minutes and 50° for 5 minutes) to distilled water (for 5 minutes) at room temperature. After rehydration, the sections were immersed for 8 min in sodium citrate buffer (pH 6) at 75°C for antigen retrieval and subsequently immersed for 8 min in acetone at −20 °C to reduce the risk of detaching sections from the slide. The immunostaining was performed using the Immunoperoxidase Secondary Detection System (Millipore, Burlington, MA, USA & Canada, cat. N° DAB-500). Then the sections were washed with PBS and treated with 3% hydrogen peroxide for 10 minutes to inhibit the endogenous peroxidases. After another wash with PBS, the sections were covered by drops of blocking reagent for 5 minutes in a humid chamber before incubation with primary antibody overnight at 4°C. The primary antibodies were used anti-NF-κB (mouse monoclonal antibody, Santa Cruz Biotechnology, Dallas, TX, USA, E10, sc-8414, dilution 1:150), anti-Nfr2 (rabbit polyclonal antibody, NOVUS BIO-Techne Abingdon, United Kingdom, NBP1–32822 dilution 1:200), anti-Occludin (rabbit polyclonal antibody, Santa Cruz Biotechnology, Dallas, TX, USA, H279, sc-5562, dilution 1:200). The day after, the sections were rinsed with Rinse Buffer for 30 seconds and incubated with secondary antibody for 10 minutes at room temperature. After another wash with buffer, the sections were incubated with Streptavidin HRP for 10 minutes at room temperature and then, with a sufficient volume of Chromogen Reagent for 10 minutes in the dark. Subsequently, another buffer wash was performed before the incubation with Hematoxylin solution for nuclear counterstaining. At the end of the reaction, the slides were mounted with coverslips using a permanent medium (Vecta Mount, H-5000, Vector Laboratories, Inc., Burlingame, CA, USA). For the immunopositivity evaluation, the slides were observed with an optical microscope (Microscope Axioscope 5/7 KMAT, Carl Zeiss, Milan, Italy) connected to a digital camera (Microscopy Camera Axiocam 208 color, Carl Zeiss, Milan, Italy) to take pictures. The immunomorphological evaluation was performed by two independent observers on two separate occasions to give a quantitative analysis in percentage of immunopositivity. To calculate the percentage of immunopositivity, all evaluations were made at high-power-field (HPF, magnification 400x) and repeated for 10 HPFs.

### 2.15. Western blot

Protein lysates were prepared from colon biopsies as described in other studies [49]. Each sample was homogenized with protein lysis buffer (Tris-HCl pH 7.6 50 mM, NaCl 300 mM, TritonX-100 0.5%, PMSF 1X, leupeptin 1X, aprotinin 1X, phosphatase inhibitors 1X (Phosphatase inhibitor cocktail 10X) and $H_2O$ milliQ) using a mechanical homogenizer. Samples were kept overnight in a shaker at 4°C and then centrifuged at 14000 g for 20 minutes at 4°C. Protein quantification was carried out by Bradford assay and the reading was executed on the bio-photometer at a wavelength of 595 nm. Protein lysates (30 μg in a total volume of 30 μl) were analyzed by SDS-PAGE followed by western blotting. Antibodies used were: Anti-Nrf2; anti-NF-κB p65 (Novus Biologicals), anti-β-actin (Santa Cruz Biotechnology, CA, USA). Membranes were incubated with HRP-conjugated secondary antibody (Thermo Fisher Scientific, Cambridge, MA, USA). Chemiluminescence was detected using the Amersham ECL Western Blotting Detection Reagent (GE Healthcare Life Sciences) chemiluminescence solution. The signal detection was performed with the Chemidoc (Biorad, Milan, Italy).

### 2.16. Fecal bacteria DNA extraction, sequencing and bioinformatics

Fecal bacterial DNA was extracted using the QIAamp PowerFecal Pro DNA Kit (Qiagen, Hilden, Germany,) and a bead homogenizer (Bullet Blender Storm, Next Advance, Averill Park, NY). A DNA fragment comprising the V3 and V4 hypervariable regions of the 16 s rRNA gene was amplified for sequencing analysis. Amplicons were sequenced on the MiSeq Illumina platform (Illumina, San Diego, CA). Sequence analyses and data quality filtering were performed with QIIME2 v.2023.5 [50] and reads were assigned to Amplicon Sequence Variant (ASV) using DADA2 [51]. Taxonomic classification was obtained using classify-sklearn, a Scikit-Learn method [52]. The weighted classifier was constructed from Silva Database v. 138.1 including region V3-V4 and the weighted information was downloaded from readytowear (https://github.com/BenKaehler/readytowear [53]). Sequences that did not match any reference were discarded. Rarefaction was used to normalized data and alfa and beta diversity indexes were calculated. Differences in alfa indexes (Shannon index, Observed features, Evenness and the Faith's phylogenetic diversity index) were analyzed using the Kruskal-Wallis test, and the p-values were adjusted with the Benjamini-Hochberg false discovery rate (FDR) [54]. The β-diversity microbiota indexes (Bray-Curtis index, Jaccard similarity index, unweighted Unifrac, and weighted unifrac) were analyzed by the Permutation Based Analysis of Variance (PERMANOVA) with the p-values adjusted by the FDR (q-value). To identify bacterial taxa differentially represented between groups Analysis of Compositions of Microbiomes with Bias Correction (ANCOM-BC) was performed using R 4.3.1 and ANCOMBC package v. 2.2.2.

### 2.17. Statistical analysis

*In vitro* experiments: data are reported as mean ± standard deviation (SD) of biological replicates. Statistical analysis was performed using GraphPad Prism software (GraphPad software, Inc., La Jolla, CA). The normal data distribution was assessed by the Shapiro-Wilk test. When data followed normal distribution, the statistical significance of the differences was analyzed using a two-tailed Student's t-test; otherwise, a non-parametric method (Mann-Whitney test) was used to compare the groups. A p-value $\leq 0.05$ was considered significant. The statistical details of each experiment can be found in the figure legends.

*In vivo* experiments: all data are means ± SEM. Statistical analysis was performed using GraphPad Prism software, utilizing One-way

ANOVA and Dunnett's multiple comparison test, and considered significant if the p-value was $<0.05$.

## 3. Results

### 3.1. Characterization of industrially-produced lemon nanovesicles (iLNVs)

Nanoparticle tracking analysis (NTA) revealed that the iLNVs have a homogeneous size distribution, with a mean of 172.8 +/- 0.3 nm and a mode of 146.5 +/- 12.6 nm (Fig. 2A). Scanning electron microscopy analysis showed that iLNVs had typical round shapes (Fig. 2B), and the measured sizes were consistent with the NTA analysis. In addition, the 30 compounds listed in Table 3 were identified in iLNVs by the use of LC-UV-MS /MS (Fig. 2C). These compounds include flavonoids and organic acids, such as hesperidin, eriocitrin, quercetin, and rutin, known in the literature for their anti-inflammatory, antioxidant, antidiabetic, anticancer, antibacterial, and antiviral effects [55,56]. Quantitative analysis by LC-MS/MS of the five most abundant identified analytes was also performed: Eriocitrin, Hesperidin, Luteolin-7-rutinoside, Citric acid, and Isocitric acid. The data obtained, expressed as mg/mL, are shown in Supplementary Table 1.

### 3.2. Anti-inflammatory effects of iLNVs on THP1 M0 macrophages

In our previous studies, we already demonstrated the ability of lemon-derived nanovesicles (LNVs) to counteract inflammatory conditions *in vitro*, *ex vivo*, and *in vivo* [28,41]. Here, to ensure that the industrial scale-up process allows us to obtain nanovesicles with preserved anti-inflammatory capability, we first tested their effects on human macrophages (THP1 M0 cells). The results, reported in Fig. 3 A, showed that cell viability was not affected by the exposure to 2.5 and 5 μg/mL of

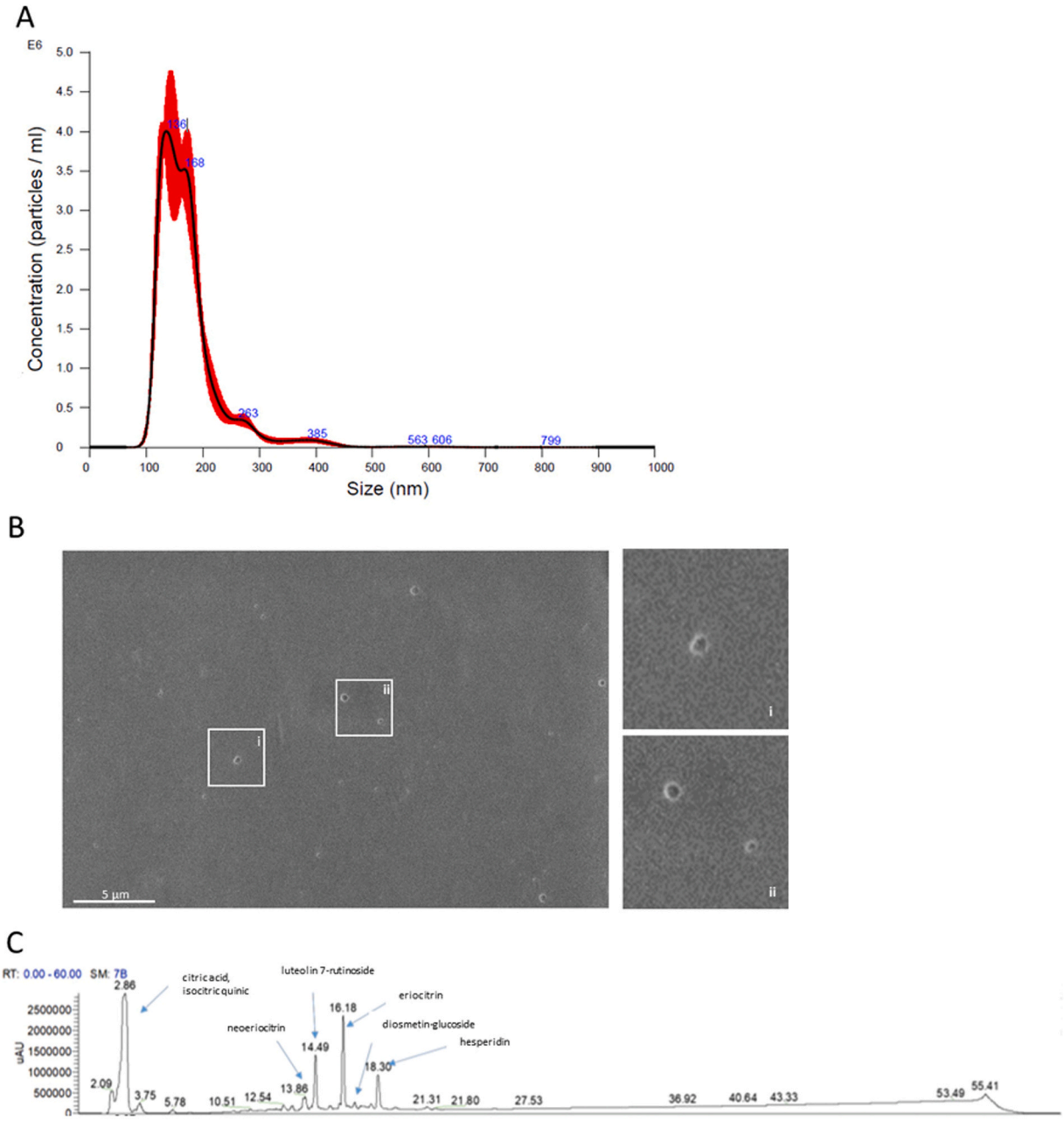


**Fig. 2. :** iLNVs characterization. (A) Size distribution of iLNVs obtained through NTA. (B) Representative image of scanning electron microscopic (SEM) analysis. (C) Qualitative analysis of the iLNVs using LC-UV-MS /MS.

**Table 3**
Composition of iLNVs. The table includes chemical class, molecular formula, and molecular weight.

| NAME | CHEMICAL CLASS | FORMULA | MW |
|---|---|---|---|
| Isocitric acid | organic acid | C6H8O7 | 192,03 |
| Citric acid | organic acid | C6H8O7 | 192,03 |
| Noreugenin | cromone | C10H8O4 | 192,04 |
| 7-hydroxy-6-methoxy-2 H-chromen-2-one | coumarins | C10H8O4 | 192,04 |
| D-(-)-Quinic acid | organic acid | C7H12O6 | 192,06 |
| Myristycin | Benzodioxoles | C11H12O3 | 192,08 |
| (+/-)-Eriodictyol | Flavonoid | C15H12O6 | 288,06 |
| Dihydrokaempferol | Flavonoid | C15H12O6 | 288,06 |
| 5,7-dihydroxy-2-(2,3,4-trihydroxyphenyl)-4 H-chromen-4-one | Pentahydroxyflavone | C15H10O7 | 302,04 |
| Quercetin | Flavonoid | C15H10O7 | 302,04 |
| 5-Deoxymyricetin | Flavonoid | C15H10O7 | 302,04 |
| L-Glutathione (reduced) | Tripeptide | C10H17N3O6S | 307,08 |
| Isorhamnetin | Flavonoid | C16H12O7 | 316,06 |
| Luteolin-6-C-glucoside | Flavone | C16H12O7 | 316,06 |
| Obacunone | Limonoid | C26H30O7 | 454,2 |
| Diosmetin-glucoside | Flavonoid | C22H22O11 | 462,12 |
| Limonin | Limonoid | C26H30O8 | 470,19 |
| Naringin | Flavonoid | C27H32O14 | 580,18 |
| Cyanidin 3-O-rutinoside | Anthocyanin | C27H30O15 | 594,16 |
| Eriocitrin | Flavanone glycoside | C27H32O15 | 596,17 |
| Neoeriocitrin | Flavanone glycoside | C27H32O15 | 596,17 |
| Diosmin | Flavonoid | C28H32O15 | 608,17 |
| Neodiosmin | Flavanone glycoside | C28H32O15 | 608,17 |
| Diosmin like compound | Flavanone glycoside | C28H32O15 | 608,17 |
| Luteolin-3′,7-Diglucoside | Flavanone glycoside | C27H30O16 | 610,15 |
| Rutin | Flavanone glycoside | C27H30O16 | 610,16 |
| Hesperidin | Flavanone glycoside | C28H34O15 | 610,19 |
| Luteolin-rutinoside | Flavanone glycoside | C27H30O15 | 616,14 |
| Kampherol-neohesperoside | Flavanone glycoside | C27H30O15 | 616,14 |
| Limonin glucoside | Furanolactone | C32H42O14 | 650,26 |

iLNVs. To test the anti-inflammatory effects of iLNVs were analysed the expression of IL-6, TNF-α, and IL-10. The results showed that, the pre-treatment of human macrophages with 5 μg/mL of iLNVs for 24 h significantly reduced the expression of the pro-inflammatory cytokines IL-6 and TNF-α induced by LPS exposure, while increased the levels of the anti-inflammatory cytokine IL-10 (Fig. 3B, upper panel). These results were also confirmed at the protein level by ELISA assay (Fig. 3B, lower panel). Overall, these data are in line with those previously reported and demonstrate that iLNVs exert anti-inflammatory activity by counteracting the effects of LPS.

### 3.3. Effects of iLNVs on colitis-related symptoms in DNBS-treated rats

The anti-inflammatory properties observed *in vitro* were then explored *in vivo* in rats with colitis experimental induced by DNBS, a well-known animal model for studies related to chronic inflammatory bowel diseases [57]. iLNVs were administered by oral gavage once a day for 14 days starting 7 days before the induction of colitis.

DNBS administration in rats induced an intestinal inflammatory process scored by DAI, clinically characterized by the presence of loose stools or diarrhea, blood in feces, and weight loss of more than 5% starting by day 2 following the DNBS injection. There were no changes in body weight gain or in stool consistency in the sham group (Fig. 4A). Pre-treatment with iLNVs (0.6 mg/kg) for 7 days before the colitis induction, promoted a significant relief of the clinical signs, in particular in rectal bleeding or diarrheic condition, leading to the reduction in the DAI values when compared to the DNBS treatment ($p < 0.05$) (Fig. 4A).

After the sacrifice, the macroscopic damage score (Fig. 4B) was used to evaluate the severity of the inflammatory conditions. In the colitis group (DNBS) an intense mucosal injury, increased wall thickness, hyperemia, ulceration, edema, and necrosis were observed, leading to high macroscopic score (Fig. 4B). DNBS rats also revealed a significant decrease in colon length and increase of colon weight, an index of oedema tissue. iLNVs pre-treatment decreased the DNBS-induced macroscopic changes by reducing the inflammation symptoms in colon tissues such as mucosal injury and the size of the ulcer area. Diffuse adhesions of the colon with other organs, typically observed during the acute phase of colitis, were unremarkable and only sporadically observed in iLNVs-pre-treated animals. In addition, beneficial effects of iLNVs on the inflammatory process were observed, partially recovering the colon shrinkage and reducing the weight/length (Fig. 4C). Thus, both the DAI and macroscopic data reveal an attenuated inflammatory process in iLNVs-treated animals.

### 3.4. Effects of iLNVs on histopathological changes in inflamed colon tissue and myeloperoxidase activity

A very common feature in colitis is the presence of a conspicuous inflammatory infiltrate [58–60]. In colon tissue, this is associated with elevated levels of myeloperoxidase (MPO), a lysosomal enzyme produced by neutrophils and macrophages and released by them as a consequence of inflammatory conditions [61]. MPO also actively generates reactive oxygen species (ROS) and is therefore associated with oxidative stress processes [62]. As expected, the colonic myeloperoxidase activity was increased in the DNBS-treated animals when compared to the sham group (Fig. 5A). These data were confirmed by histological analysis of the collected colon tissues. The histological alteration was evaluated by hematoxylin-eosin (H&E) staining of colonic tissues as shown in Fig. 5B. It was discernible that the normal tissue architecture in healthy animals (Fig. 5B Sham and iLNVs) had some random inflammatory cells (this observation is still normal, Fig. 5B, green arrows). In contrast, the animals with colitis (Fig. 5B DNBS) had a different tissue morphology, which was completely subverted in its glandular architecture (Fig. 5B, blue arrows) by the severe inflammatory infiltrates (Fig. 5B, red arrows). This condition was ameliorated in animals pre-treated with iLNVs (Fig. 5B iLNVs +DNBS) where a restoration of glandular architecture (Fig. 5B, yellow arrows) and a decrease in inflammatory infiltrate was observed. Overall, the pre-treatment with iLNVs protects colon tissue by colitis-induced damages.

### 3.5. Anti-inflammatory and antioxidant properties of iLNVs in rats

Molecular analysis from colon explants allowed us to confirm the *in vitro* data, and to evaluate the anti-inflammatory properties of iLNVs in our rat model. The analysis revealed that DNBS treatment causes a significant increase in IL-6 expression in the DNBS group of animals compared to the sham group. This increase was significantly prevented by pre-treatment with iLNVs (iLNVs+/DNBS+) (Fig. 6A). To investigate the molecular pathway underlying the observed *in vivo* anti-inflammatory effect, we first examined the expression of NF-κB, the master regulator of inflammatory processes, in colon tissue. Western blot analysis showed that the expression of NF-κB was slightly increased in the DNBS animals compared to the sham group. This effect was limited by pre-treatment with iLNVs (Fig. 6B). NF-κB was also evaluated by immunohistochemistry. The results, consistent with the trend observed by the western blot, attribute significance to the data. As shown in Fig. 6C, there was a significant increase in the percentage of cells positive for NF-κB in the colon tissue of colitic rats (iLNVs-/DNBS+) compared to the sham group; this percentage decreases significantly in the colitic animals pre-treated with iLNVs (iLNVs+/DNBS+).

Further, the molecular pathway associated with oxidative stress was also evaluated. The expression of Nuclear factor-erythroid 2-related factor 2 (Nrf2), the upstream regulator of genes involved in the neutralization of oxidative stress, was analyzed by Western blot. As shown in Fig. 7A, there was a significant increase in Nrf2 levels in the two rat groups treated with iLVNs (iLNVs+/DNBS-; iLNVs+/DNBS+) compared to the group with colitis (DNBS). In addition,

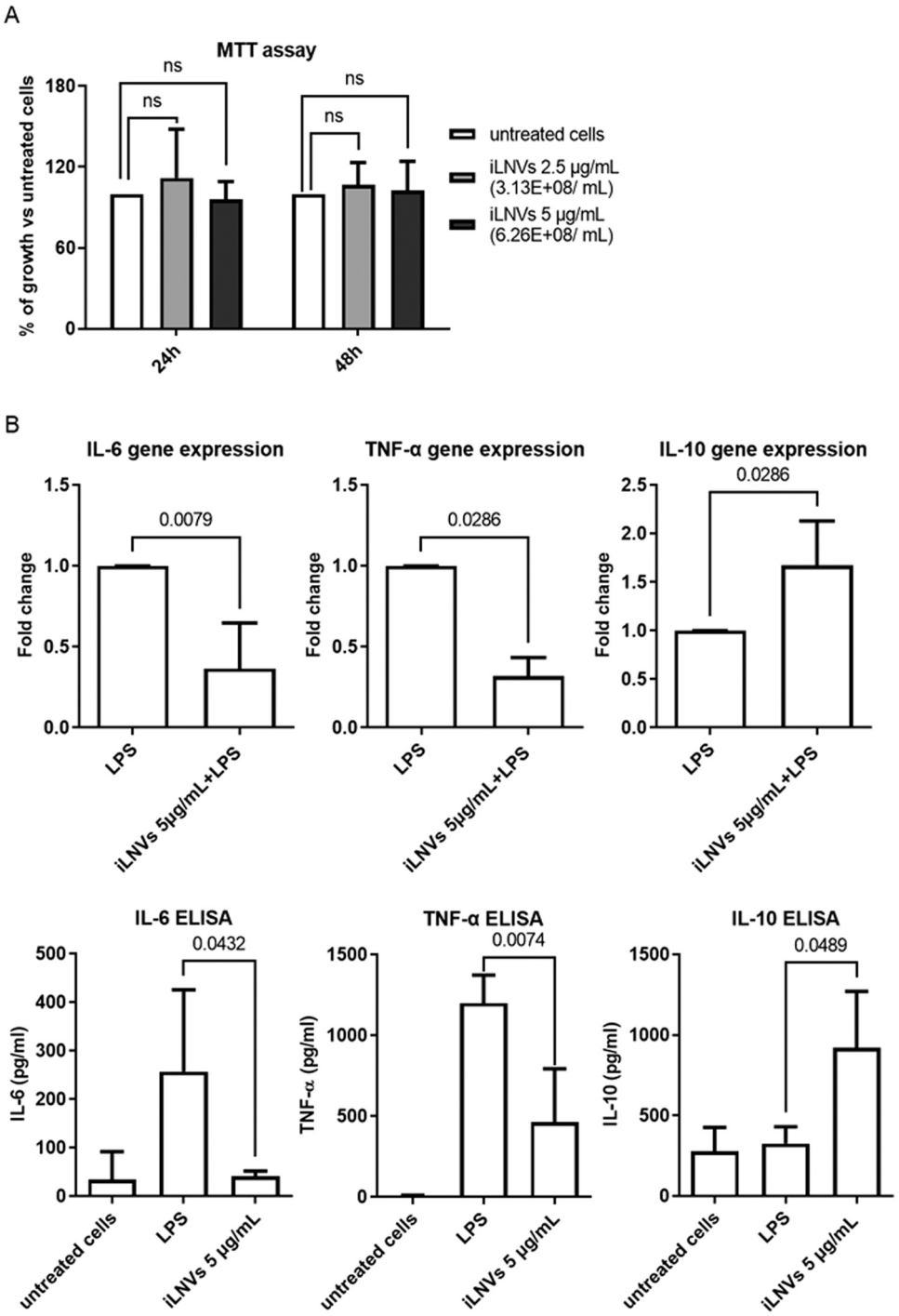


**Fig. 3.** (A) THP1 M0 cell viability after exposure to iLNVs. Cell viability was measured by MTT assay after 24 and 48 h of treatment with 2.5 and 5 µg/mL of iLNVs. The values were plotted as the percentage of cell viability versus untreated cells. Values are the mean ± SD of three biological replicates. (B) The anti-inflammatory effects of iLNVs on the transcript levels of IL-6, TNF-α, and IL-10 were evaluated by qRT-PCR analysis. THP1 M0 cells were treated for 24 h with iLNVs (5 µg/mL) and then exposed to LPS 1000 ng/mL for 3 h. Values are reported as fold changes compared with LPS-treated cells and are the mean ± SD of three biological replicates (upper panel). The level of IL-6, TNF-α, and IL-10 proteins was measured by ELISA in the conditioned medium of THP1 M0 cells treated as specified above. Values are the mean ± SD of three biological replicates (lower panel).

immunohistochemical analysis of the colon tissues (Fig. 7B) reveals that in the DNBS-treated group, Nrf2 is mainly cytoplasmic; in contrast, its localization is predominantly nuclear in animals pre-treated with iLNVs. Thus, iLNVs appear to exert an antioxidant effect increasing Nrf2 nuclear levels.

### 3.6. *Effect of iLNV treatments on tight junctions*

In pathological conditions, including IBD, the permeability of the intestinal epithelium is compromised, and this is due to a reduction of tight junctions [63–65]. For this reason, we first analyzed the Occludin mRNA level in the colon tissue samples. The histogram in Fig. 8A shows a significant reduction in Occludin expression in the DNBS-treated

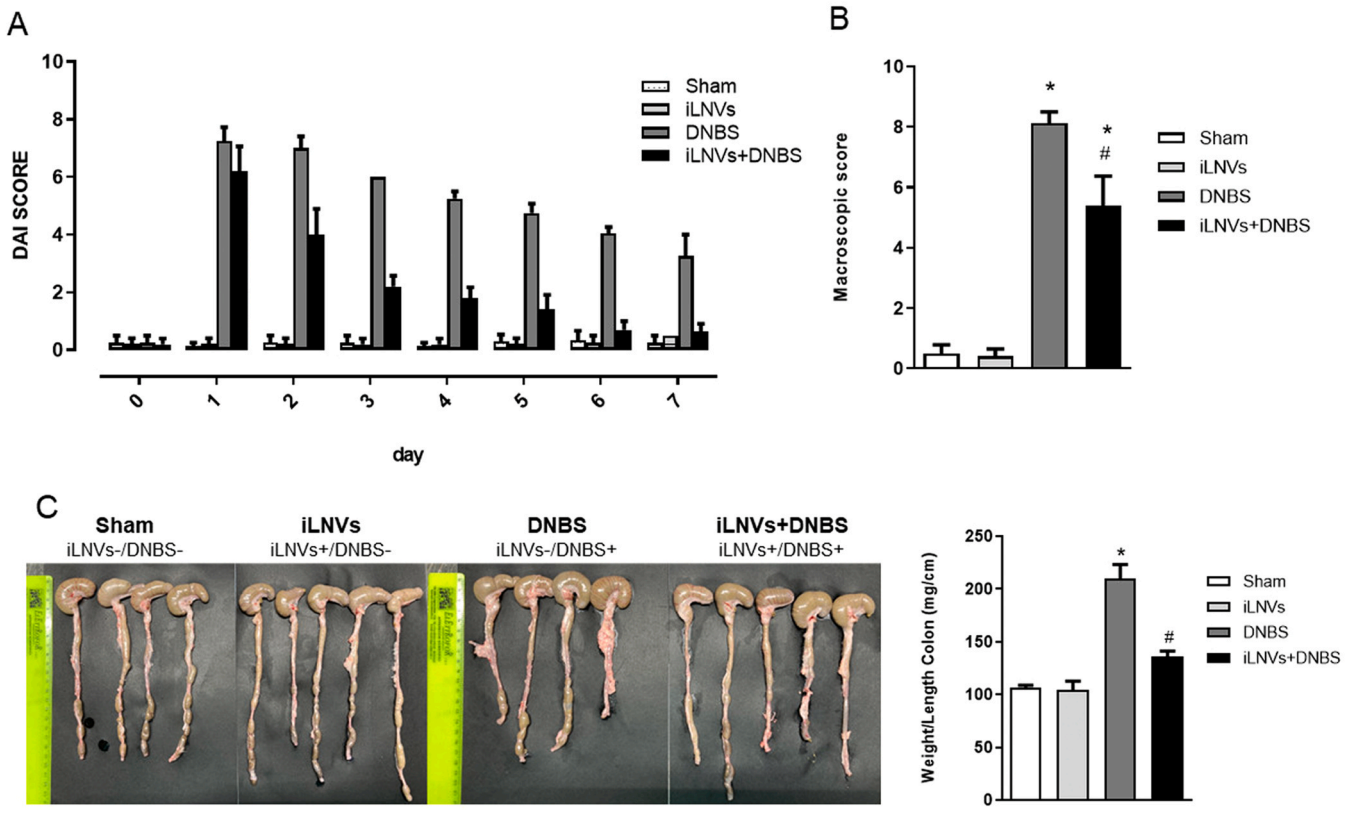


**Fig. 4. :** iLNVs ameliorated colitis-related symptoms in DNBS-treated rats (A) DAI score evaluation and (B) macroscopic damage score. (C) *Postmortem* analyses showing the variation in colonic length a (left side) and colon weight/length ratio (right side) in four groups of animals. Data are mean ± SEM (n= 4–5 for each group). *P < 0.05 versus Sham group, #P < 0.05 versus DNBS group.

animals compared to the sham group, while a significative recovery can be observed in the group of animals with colitis, pre-treated with iLNVs (iLNVs+/DNBS+). These results were confirmed by immunohistochemistry. The images in Fig. 8B show that the immunopositivity for Occludin (indicated with arrows) found in sham group and iLNVs group is almost absent in DNBS-treated cases while it is again observed in the iLNVs-pretreated colitic animals (iLNVs+/DNBS+). These results suggest that treatment with iLNVs may attenuate the effects of DNBS by acting on tight junction expression and reducing the impaired intestinal permeability characteristic of IBD.

### 3.7. iLNVs administration modulates the gut microbiota

The composition and diversity of the gastrointestinal microbial community play a crucial role in gut health and IBD pathogenesis; therefore, here we analyzed the changes in the gut microbiota in the four different groups. The analysis of the beta-diversity of microbiota samples showed no differences in the Bray-Curtis index, observed species, and in the weighted and unweighted Unifrac indexes. The composition of the fecal microbiota exhibited significant differences in the Jaccard Dissimilarity index (Fig. 9) between Sham and DNBS (q-value 0.042), DNBS and iLNVs + DNBS (q-value 0.042), and iLNVs and iLNVs + DNBS (q-value 0.015). The Jaccard index, which assesses species presence/absence regardless of abundance, indicated that induced inflammation led to changes in the presence of specific bacterial taxa, particularly following treatment with iLNVs.

When alfa diversity was analyzed (Faith's index, Shannon index, Observed features, Pielou eveness) analyses revealed no significant changes in the microbiota between the four analyzed groups (Supplementary Figure 1).

The analyses at the genus level unveiled significant alterations in the microbiota composition. In the DNBS-treated group (Fig. 10), there was an increased representation of *Pygmaiobacter*, *Lachnospiraceae*_UCG-010, *Tuzzerella*, and *Anaerofilum* genera alongside a decreased marked representation of the *Enterococcus* and *Bacteroides_pectinophilus* group. These changes were not observed in the colitis group pre-treated with iLNVs (iLNVs + DNBS) (Fig. 10), indicating that iLNVs treatment may somehow counteract the effects of inflammation on the gut microbiota, even causing an opposite effect as in the case of the genus *Anaerofilum*. Moreover, in the colitis-induced group treated with iLNVs an elevated presence of *Lachnospiraceae NK4B4* was also observed along with a decreased presence of *Enteractinococcus*, and *Acetatifactor*. The administration of iLNVs alone resulted in an elevated presence of *Gordonibacter*, *Eubacterium_branchy* group, *Oscillospiraceae* UCG-005, *Oscillospiraceae* NK4A214, and *Oscillospirales* UCG-010, while *Negativibacillus* genus showed a decrease (Fig. 10).

## 4. Discussion

The benefits of citrus fruits and its by-products have always been appreciated and recognized worldwide. Their properties are due to content of the nutrients and bioactive molecules such as vitamins, carbohydrates, minerals, and dietary fibers giving them high nutritional values and, flavonoids, carotenoids, and limonoids exerting various health benefits [66–69]. However, the use of such substances in clinical practices is limited for multiple reasons such as extraction processes, storage conditions, and labile stability [70–72]. Plant-derived vesicles concentrate and carry a multitude of healthful compounds naturally present in plants, while simultaneously protecting them from external degradative and oxidative events. In addition to their natural origin, non-toxic, and low immunogenic characteristics, the possibility of isolating from large volumes makes them even more attractive [31]. In our previous work, we have demonstrated the anti-inflammatory and antioxidant properties of lemon-derived nanovesicles *in vitro* and *ex vivo* settings [25,28,41].

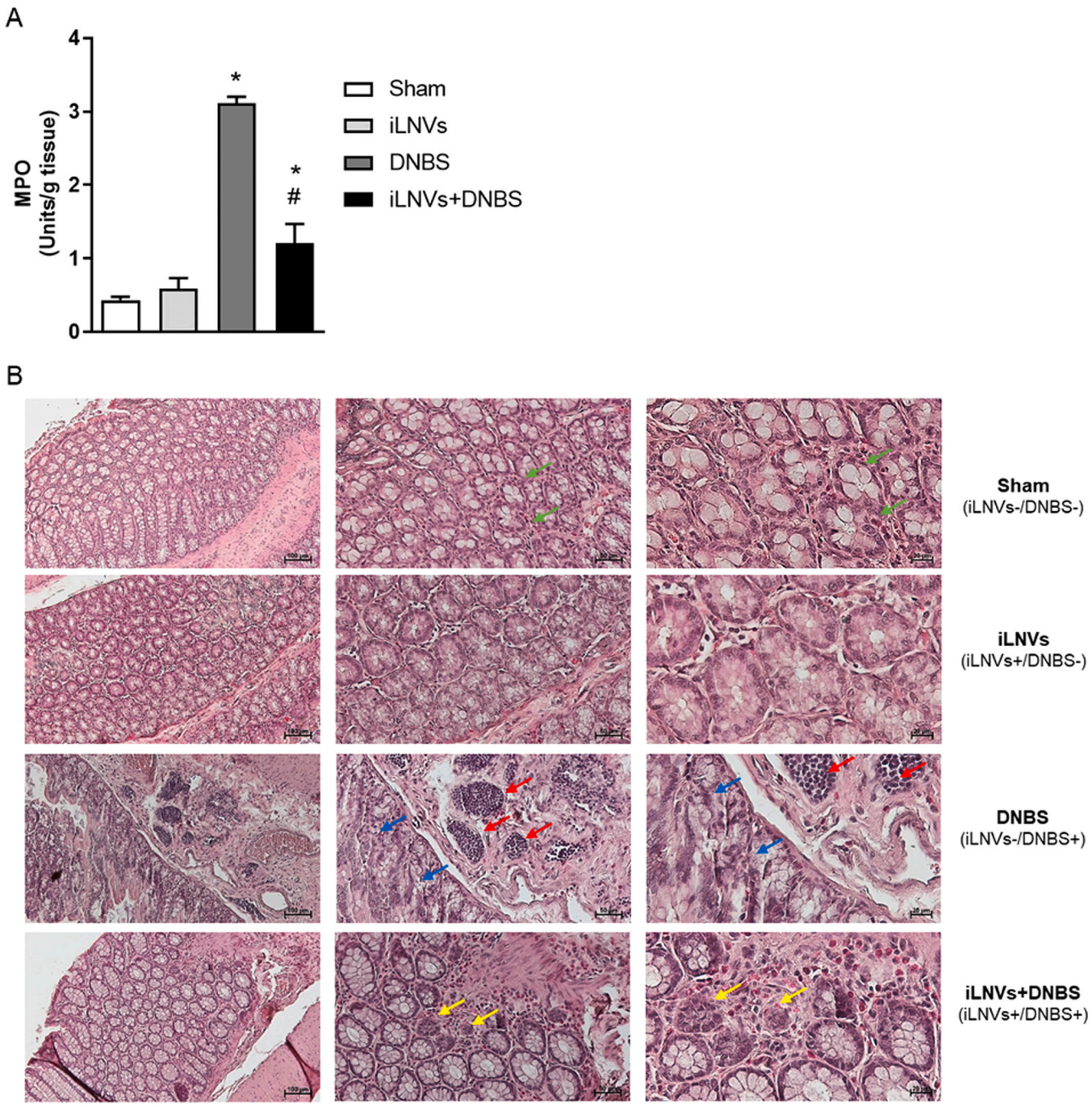


**Fig. 5. :** Myeloperoxidase activity and histological features in colonic tissues from the four groups of animals. (A) Colon MPO activity in Sham, DNBS or iLNVs -treated rats with or without colitis induction. Data are mean ± SEM (n= 4 for each group). *P < 0.05 versus control group, #P < 0.05 versus DNBS group. (B) Representative images of colon sections stained with H&E showing histological alteration and effect following iLNV treatment. Magnification of 100x, scale bar 100 μm for the images in the left column, magnification of 200x, scale bar 50 μm for the images in the center column, magnification of 400x, scale bar 20 μm for the images in the right column.

Here, we aim to evaluate eventual beneficial effects of lemon-derived nanovesicle treatment on colonic inflammation in DNBS rat, animal model widely used in IBD studies. The rationale came by the observations of the significant side effects and modest results for long-term current IBD therapies and from the evidence that diet and nutritional factors could play a key role in IBD [15,73,74]. In addition, we used a product obtained at an industrial scale, getting ever closer to the possibility of making plant vesicles a product accessible to all. Here we characterize iLNVs in terms of size, content, and morphology, demonstrating the presence of small particles with a size of less than 200 nm. Analysis of their contents revealed an overlapping profile of bioactive compounds to the laboratory-scale isolated vesicles studied in our previous work [25,28,41]. We confirm the presence of flavonoids, secondary metabolites of plants with recognized beneficial properties for human health and for their marked anti-inflammatory and antioxidant activity [75,76]. Subsequently, after confirming their safety by testing their non-interfering ability on human macrophage THP1 cell viability, we confirmed their anti-inflammatory effect *in vitro* through the reduced expression and release of the pro-inflammatory cytokines IL-6 and TNF-α and the increased levels of the anti-inflammatory IL-10. This

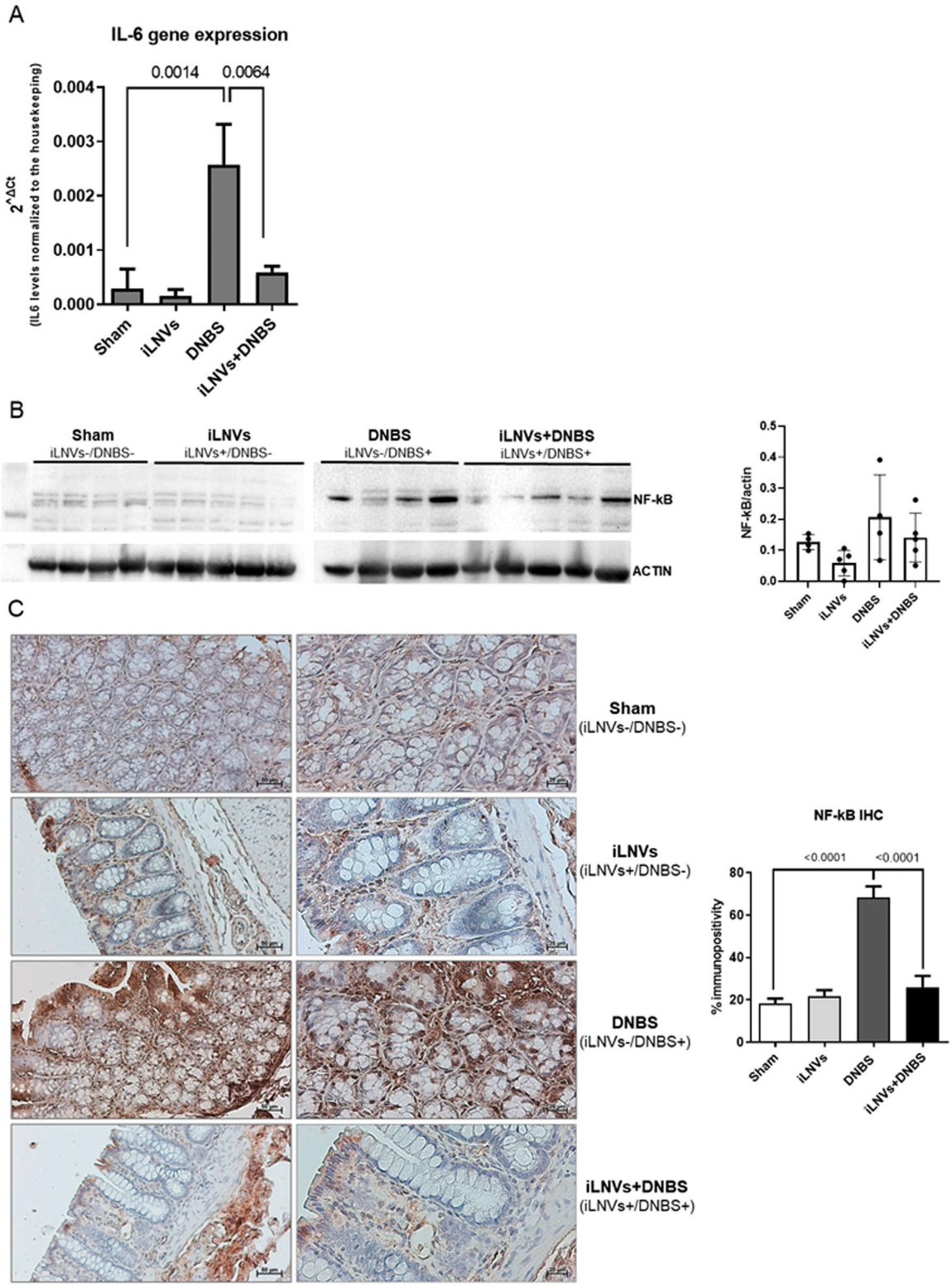


**Fig. 6. :** *In vivo* anti-inflammatory properties of iLNVs. (A) IL-6 expression levels were assessed in the colon tissue of different animal groups by qRT-PCR analysis. The value was expressed as IL-6 levels normalized to the housekeeping gene, actin ($2^{\hat{}\,\Delta Ct}$). Results are expressed as means±SD of three to four rats for each group. (B) Western blot analysis of NF-κB expression in colon tissue of different animal groups (left panel) and the relative densitogram (right panel). (C) Representative images of immunohistochemical results for NF-κB in colon tissue of different groups. Magnification 200x, scale bar 50 μm for the images on the right, magnification 400x, scale bar 20 μm for the images on the left. To calculate the percentage of immunopositivity, all evaluations were made at high-power-field (HPF, magnification 400x). The histogram shows the results of the immunohistochemical evaluations. The data are means±SD of ten evaluations for each group.

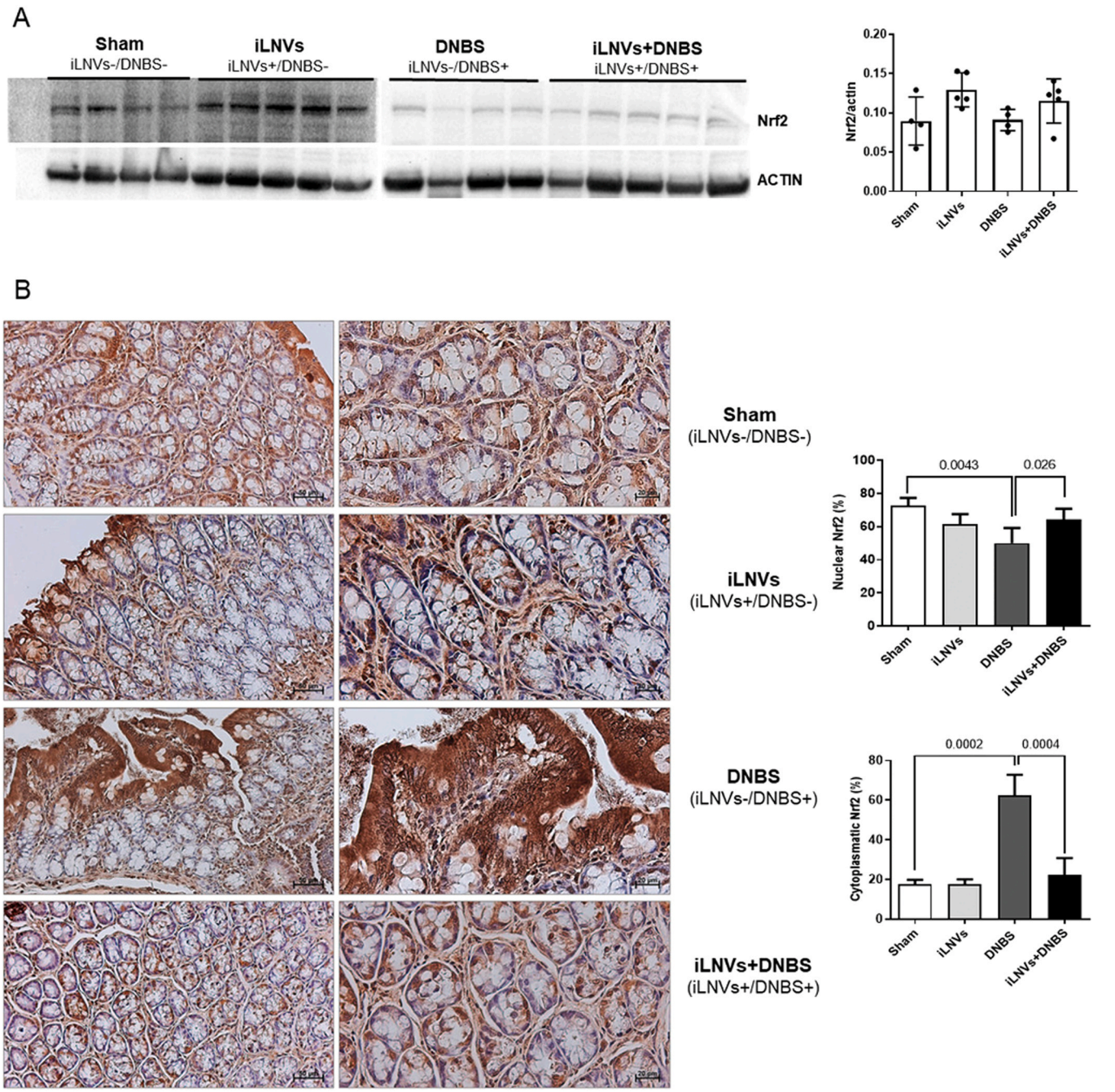


**Fig. 7. :** *In vivo* antioxidant properties of iLNVs. (A) Western blot analysis of Nrf2 expression in colon tissue of different animal groups (left panel) and the relative densitogram (right panel). (B) Representative images of immunohistochemical results for Nrf2 in colon tissue of different groups. Magnification 200x, scale bar 50 μm for the images on the right, magnification 400x, scale bar 20 μm for the images on the left. To calculate the percentage of immunopositivity, all evaluations were made at high-power-field (HPF, magnification 400x). The istogram shows the results of the immunohistochemical evaluations. The data are means±SD of ten evaluations for each group.

finding suggests that despite the two different isolation methods, iLNVs maintain the same biological properties as lemon-derived vesicles isolated on a laboratory scale [25,28,41]. *In vivo* studies investigated the use of plant-derived nanovesicles as traditional orally administered drugs for the treatment of many diseases. Among the latest, yam-derived exosome-like nanovesicles can serve as a safe and orally effective agent in the treatment of osteoporosis [77], Beta vulgaris-derived exosome--like nanovesicle significantly alleviated chronic Dox-induced cardiotoxicity in terms of echocardiographic and histological results in mice [78] or even orange juice-derived nanovesicles could be used for the treatment of obesity-associated intestinal complications [79]. However, a handful number of research have explored the use of plant nanovesicles in the field of IBD. So, the main goal and next step was to test the effects of iLNVs treatment *in vivo* on the animal model of DNBS-induced colitis in rats.

iLNV treatment caused an improvement in the clinical signs representative of the DNBS-induced colitis (DAI score) and in the colonic weight/length ratio. Indeed, at the microscopic level, treatment with iLNVs restores the specific histological features of the colon tissue, such as tissue architecture, reduces the inflammatory infiltrate, leading to a decrease in MPO levels. Moreover, iLNVs exert anti-inflammatory and antioxidant effect and enhances tight junction proteins to improve gut

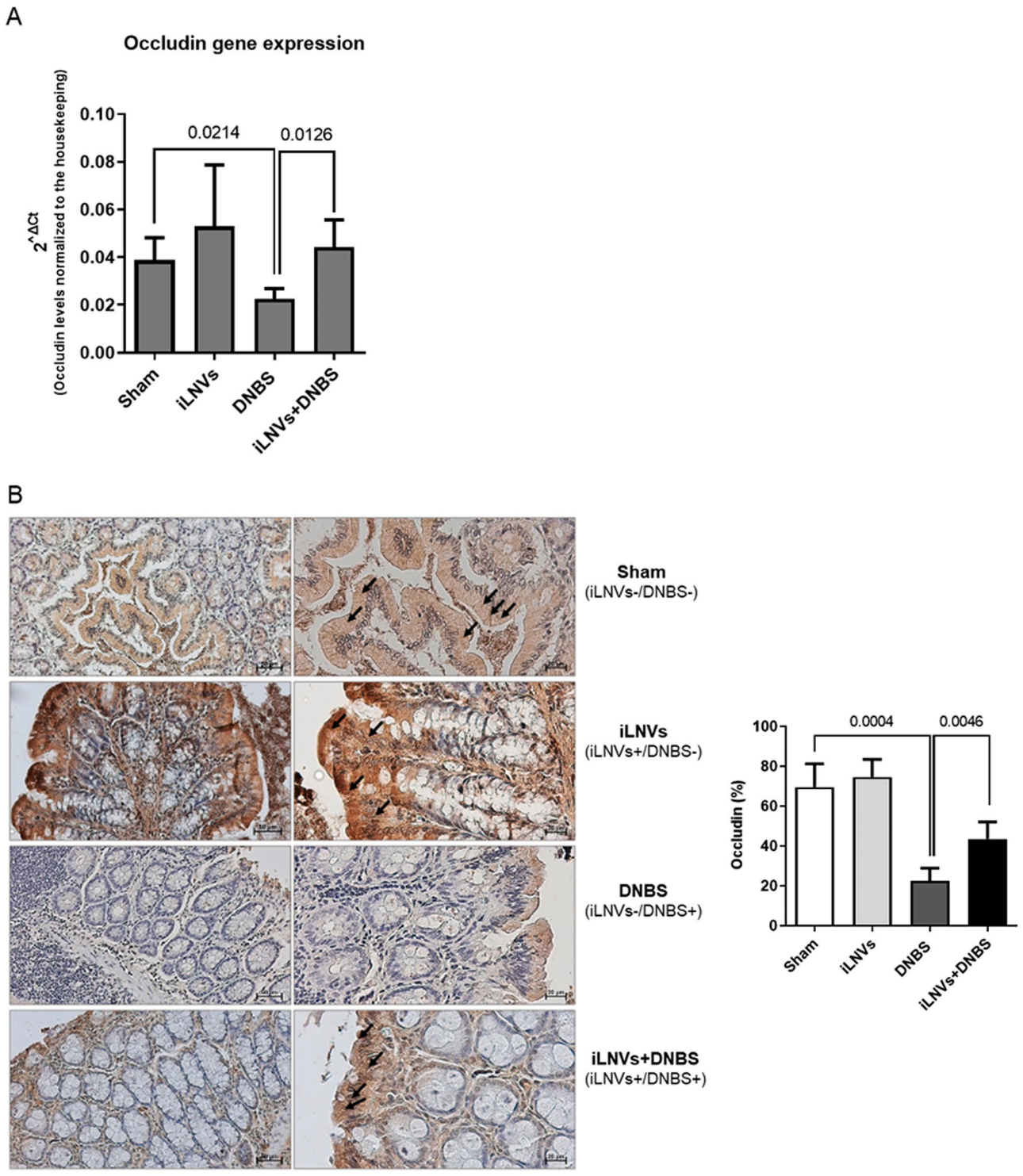


**Fig. 8. :** *In vivo* effect of iLNVs on tight junctions. (A) Occludin expression levels were assessed in the colon tissue of different animal groups by qRT-PCR analysis. The absolute target gene expression in each sample of colon tissue was expressed as $2^{-\Delta Ct}$. Gene expression was normalized by Actin. Results are expressed as means ±SD of four rats for each group. (B) Representative images of immunohistochemical results for Occludin in colon tissue of different groups. Magnification 200x, scale bar 50 μm for the images on the right, magnification 400x, scale bar 20 μm for the images on the left. To calculate the percentage of immunopositivity, all evaluations were made at high-power-field (HPF, magnification 400x). The istogram shows the results of the immunohistochemical evaluations. The data are expressed as means ±SD of ten evaluations for each group.

permeability. These observations are in line with other studies in which vesicles isolated from edible plants including grapefruit [37], turmeric [80], and garlic [81] protected the colon from DSS- or DNBS-induced damage. In this study, we attempted to correlate the observed effects with molecular pathways involved with inflammatory and antioxidant processes. iLNVs treatment can attenuate expression levels of NF-κB. NF-κB, is a redoxsensitive transcription factor, key regulator of inflammation, innate immunity, and tissue integrity. NF-κB phosphorylation and its nuclear translocation correlate with the severity of intestinal inflammation [82,83] due to the regulation of gene expression of

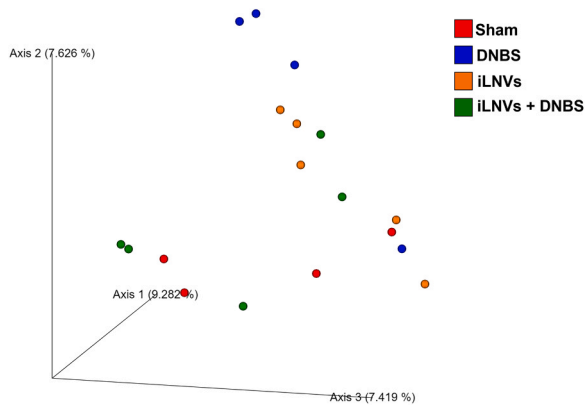


**Fig. 9. :** Principal Coordinates Analysis (PCoA) based on beta-diversity Jaccard index of the gut microbiota of the four groups analyzed. Each data point represents an individual sample.

molecules including adhesion molecules, chemokines, and cytokines [84]. We can suppose that iLNVs, inhibiting the early steps of inflammation, lead to an attenuation of DNBS-colitis features. A reduced activation of NF-kB will lead to infiltrating cells to produce a decreased amounts of inflammatory mediators and subsequently to better maintenance of mucosal integrity. At the same time, we found an increase in the expression of Nrf2, a mediator of antioxidant pathways, and a nuclear localization, in iLNVs-treated groups, suggesting that they can enhance the antioxidant response under both pathological and physiological conditions.

Moreover it is well know that epithelial tight junctions are compromised in patients or animal models with IBD [85]. Occludin is a protein component of tight junctions; its loss or reduced expression results in barrier loss and in the the increase of leak pathway permeability induced by inflammatory stimuli its removal from tight junctions. iLNVs treatment induced a rescue of Occludin expression suggesting that vesicles can improve colon permeability. However further functional studies could help to confirm these observations.

Underlying these findings, valuable compounds in which iLNVs are enriched could play an important role. Some of these such as luteolin-7-O-rutinoside [86], quercetin [87,88], hesperidin [89,90] and eriocitrin [91,92] have been extensively studied *in vitro* and *in vivo* and are well known as modulators of these processes. Finally increasing studies recognize the importance of microbiota in human health and deregulations of its balance are involved in numerous disease processes [93], especially concerning the gut. Gut microbiota promotes the differentiation of intestinal epithelial and immune cells, provides energy to the host through metabolic processes, and defends against infections caused by pathogens [94,95]. Based on these assumptions we aimed to explore this aspect by analyzing how the bacterial population changes following treatment with iLNVs. We found that DNBS-induced inflammation produced changes in some bacterial taxa compared with untreated animals and in particular a marked decrease in *Enterococcus* and *Bacteroides_pectinophilus* group.

Although an increase in the *Enterococcus* genus has been associated with the presence of IBD [96], in our case, we have observed that the DNBS group had a lower presence of this bacterial genus. The association of the *Enterococcus* genus with inflammatory bowel disease (IBD) is currently still contradictory. There are also studies indicating that inoculation with specific strains of *Enterococcus faecalis* can improve DNBS-induced intestinal inflammation [97] and induce the secretion of an endopeptidase that reduces intestinal inflammation by activating the innate immune receptor NOD2 [98]. In fact, different *Enterococcus* clades has been associated with either IBD or health [99]. The *Bacteroides pectinophilus* group, as in our study, has been previously described as enriched in samples from control patients when their microbiota was compared with that of individuals with irritable bowel syndrome (IBS) [100] and has been previously negatively correlated with inflammatory markers [101,102]. In contrast, DNBS-induced inflammation increased the *Pygmaiobacter*, *Lachnospiraceae* UCG-010, *Anaerofilum* and *Tuzzerella* genera when compared to the sham group.There are currently no studies linking the presence of the *Tuzzerella, Pygmaiobacter* or *Anaerofilum* genus with intestinal inflammation.

While the literature indicates that *Lachnospiraceae* members are prominent producers of substances with potentially positive effects on human health, such as short-chain fatty acids, various taxa are also linked to a range of intra- and extraintestinal diseases. The influence of these taxa on host physiology is frequently inconsistent among different studies [103]. The treatment with iLNVs promoted the presence of *Gordonibacter* and *Eubacterium brancy* group. The *Gordonibacter* genus has been previously associated with the metabolism of various types of polyphenols [104], so there is a possibility that the polyphenols contained in the nanovesicles may have promoted its growth. An increase in the population of *Eubacterium brancy* group has also been associated with treatment using the flavone bacalain and the alkaloid berberine, both compounds of plant origin that improved intestinal inflammation in an UC model [105]. On the other hand, decreases in the *Negativibacillus* genus, as observed in the iLNV group, have been associated with the consumption of fruit pomace fibers [106]. Finally, in the group with intestinal inflammation treated with nanovesicles, it is observed that the presence of the *Anaerofilum* genus is counteracted, reaching negative values, while no differences are observed in the rest of the species of the microbiota that had been modified by the induction of inflammation. Additionally, a decrease in the *Acetibacter* genus was detected, a genus previously associated with worsening symptoms of intestinal inflammation in a murine model [107]. Finally, the increased presence of the *Lachnospiraceae NK4B4* group could be associated with the anti-inflammatory activity observed in this study for the iLNVs, as this group is a producer of short-chain fatty acids (SCFAs), compounds known for their anti-inflammatory activity [108]. In conclusion, the modulation of the microbiota by the iLNVs, could also be a factor contributing to their anti-inflammatory effect. This aspect of the study underscores the potential role of iLNVs in modulating the gut

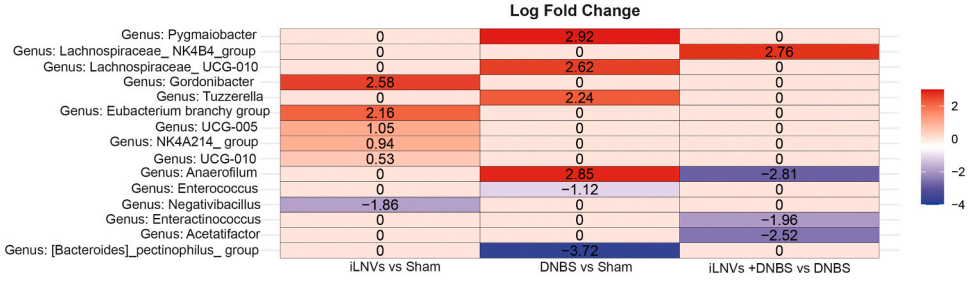


**Fig. 10. :** Heatmap of differentially abundant taxa in Sham, iLNVs, DNBS and iLNVs+DNBS identified by ANCOM-BC analysis (abundance is log-transformed). Red indicates increased abundance in the comparison group versus Sham group or DNBS group; blue indicates decreased abundance in the comparison group versus Sham group or DNBS group.

microbiota, which has emerged as a critical factor in the pathogenesis and management of IBD [109].

Overall, in this study we demonstrated for the first time that industrially produced lemon nanovesicles play a protective role *in vivo* against DNBS-induced colitis in a rat animal model 1) by modulating the expression of factors upstream of inflammatory and antioxidant processes; 2) by restoring the intestinal permeability acting on tight junctions; 3) shaping the gut microbiota.

Our findings highlight several key aspects that contribute to our understanding of the mechanisms underlying the anti-inflammatory and antioxidant properties of iLNVs and their potential implications for the treatment of inflammatory bowel disease (IBD).

## Limitations of the study

Results from this study encourage the development of lemon nanovesicles-based nutraceuticals to address intestinal chronic inflammation. clinical translation of these results needs further studies aimed at evaluating doses, timing, and mode of administration in humans considering the different complex nature of the two organisms.

## Funding

This work was fund in part by the European Union's NextGenerationEU—fondi MUR D.M. 737/2021—research project "Effetti antiinfiammatori e vasoprotettivi di vescicole extracellulari isolate da piante", EUROSTART, UNIPA, D.R. 698/2022 to Stefania Raimondo. S. R. was supported by the PON "Ricerca e Innovazione" 2014–2020-Azione 1.2 "Mobilità dei Ricercatori" of "Attraction and International Mobility" (AIM).). V.T. and R.G. are PhD students in "Biomedicina, Neuroscienze e Diagnostica Avanzata" (XXXVII ciclo) at the University of Palermo. N.R.G. is a PhD student in "Oncology and Experimental Surgery", XXXV ciclo, at the University of Palermo.

## CRediT authorship contribution statement

**Alessia Gallo:** Investigation, Data curation. **Riccardo Alessandro:** Writing – review & editing, Supervision, Funding acquisition, Conceptualization. **Alice Conigliaro:** Writing – review & editing, Writing – original draft, Methodology, Investigation, Conceptualization. **Rosa Maria Serio:** Writing – review & editing. **Maria Grazia Zizzo:** Writing – review & editing, Writing – original draft, Methodology, Investigation, Data curation. **Nima Rabienezhad Ganji:** Investigation. **Stefania Raimondo:** Writing – review & editing, Writing – original draft, Supervision, Investigation, Funding acquisition, Data curation, Conceptualization. **Mariangela Tabone:** Writing – original draft, Project administration, Methodology, Data curation. **Carlo Bressa:** Investigation, Data curation. **Adele Cicio:** Investigation. **Francesca Rappa:** Investigation, Data curation. **Mar Larrosa:** Writing – review & editing. **Roberta Gasparro:** Investigation. **Giuseppe Vergilio:** Investigation. **Vincenza Tinnirello:** Writing – original draft, Methodology, Investigation.

## Declaration of Competing Interest

The authors declare that there are no conflicts of interest that could be perceived as prejudicing the impartiality of the research reported. The authors S.R., A.C., and R.A. are cofounders of Navhetec, an Academic Spin-Off of the University of Palermo that only provide the nanovesicle extracts but that did not have any role in the conceptualization of this article and in the analysis of the results. The same authors are inventors of the Italian patents 102019000005090 and 102015902344749.

## Data Availability

Data will be made available on request.

## Acknowledgments

The authors would like to thank Dr. Sergio Nasillo from ATeN (Advanced Technologies Network) Center, University of Palermo, for Scanning Electron Microscope analysis. The authors also acknowledge the Botanicals Laboratory of Fondazione Toscana Life Sciences (Siena, Italy) for the metabolomic analysis.

### *Inclusion and diversity*

we support inclusive, diverse, and equitable conduct of research.

### *Resource availability*

Further information and requests for resources and reagents should be directed to and will be fulfilled by the lead contact, Stefania Raimondo (stefania.raimondo@unipa.it).

## Appendix A. Supporting information

Supplementary data associated with this article can be found in the online version at doi:10.1016/j.biopha.2024.116514.

## References

[1] B. Khor, A. Gardet, R.J. Xavier, Genetics and pathogenesis of inflammatory bowel disease, Nature *474* (2011) 307–317, https://doi.org/10.1038/nature10209.
[2] C. Fiocchi, Inflammatory bowel disease: complexity and variability need integration, Front. Med. *5* (2018) 75, https://doi.org/10.3389/fmed.2018.00075.
[3] K.W.J. van der Sloot, M. Amini, V. Peters, G. Dijkstra, B.Z. Alizadeh, Inflammatory bowel diseases: review of known environmental protective and risk factors involved, Inflamm. Bowel Dis. *23* (2017) 1499–1509, https://doi.org/10.1097/MIB.0000000000001217.
[4] G.P. Ramos, K.A. Papadakis, Mechanisms of disease: inflammatory bowel diseases, Mayo Clin. Proc. *94* (2019) 155–165, https://doi.org/10.1016/j.mayocp.2018.09.013.
[5] K. Yeshi, R. Ruscher, L. Hunter, N.L. Daly, A. Loukas, P. Wangchuk, Revisiting inflammatory bowel disease: pathology, treatments, challenges and emerging therapeutics including drug leads from natural products, J. Clin. Med *9* (2020), https://doi.org/10.3390/jcm9051273.
[6] T. Tian, Z. Wang, J. Zhang, Pathomechanisms of oxidative stress in inflammatory bowel disease and potential antioxidant therapies, Oxid. Med Cell Longev. *2017* (2017) 4535194, https://doi.org/10.1155/2017/4535194.
[7] A.R. Bourgonje, M. Feelisch, K.N. Faber, A. Pasch, G. Dijkstra, H. van Goor, Oxidative Stress and Redox-Modulating Therapeutics in Inflammatory Bowel Disease, Trends Mol. Med *26* (2020) 1034–1046, https://doi.org/10.1016/j.molmed.2020.06.006.
[8] F. Biasi, G. Leonarduzzi, P.I. Oteiza, G. Poli, Inflammatory bowel disease: mechanisms, redox considerations, and therapeutic targets, Antioxid. Redox Signal *19* (2013) 1711–1747, https://doi.org/10.1089/ars.2012.4530.
[9] G. Mandalari, C. Bisignano, T. Genovese, E. Mazzon, M.S. Wickham, I. Paterniti, S. Cuzzocrea, Natural almond skin reduced oxidative stress and inflammation in an experimental model of inflammatory bowel disease, Int Immunopharmacol. *11* (2011) 915–924, https://doi.org/10.1016/j.intimp.2011.02.003.
[10] D.C. Baumgart, W.J. Sandborn, Inflammatory bowel disease: clinical aspects and established and evolving therapies, Lancet *369* (2007) 1641–1657, https://doi.org/10.1016/S0140-6736(07)60751-X.
[11] S. Collingwood, J. Witherington, Therapeutic approaches towards the treatment of gastroinstestinal disorders, Drug N. Perspect. *20* (2007) 139–144, https://doi.org/10.1358/dnp.2007.20.2.1113595.
[12] K.O. Chudy-Onwugaje, K.E. Christian, F.A. Farraye, R.K. Cross, A State-of-the-Art Review of New and Emerging Therapies for the Treatment of IBD, Inflamm. Bowel Dis. *25* (2019) 820–830, https://doi.org/10.1093/ibd/izy327.
[13] Z. Cai, S. Wang, J. Li, Treatment of Inflammatory Bowel Disease: A Comprehensive Review, Front Med (Lausanne) *8* (2021) 765474, https://doi.org/10.3389/fmed.2021.765474.
[14] A.T. Abegunde, B.H. Muhammad, T. Ali, Preventive health measures in inflammatory bowel disease, World J. Gastroenterol. *22* (2016) 7625–7644, https://doi.org/10.3748/wjg.v22.i34.7625.
[15] R. Reddavide, O. Rotolo, M.G. Caruso, E. Stasi, M. Notarnicola, C. Miraglia, A. Nouvenne, T. Meschi, G.L. De' Angelis, F. Di Mario, G. Leandro, The role of diet

in the prevention and treatment of Inflammatory Bowel Diseases, Acta Biomed. *89* (2018) 60–75, https://doi.org/10.23750/abm.v89i9-S.7952.
[16] N. Iglesias, E. Galbis, M.J. Diaz-Blanco, R. Lucas, E. Benito, M.V. de-Paz, Nanostructured Chitosan-Based Biomaterials for Sustained and Colon-Specific Resveratrol Release, Int J. Mol. Sci. *20* (2019), 10.3390/ijms20020398.
[17] H. Qiao, D. Fang, J. Chen, Y. Sun, C. Kang, L. Di, J. Li, Z. Chen, Y. Gao, Orally delivered polycurcumin responsive to bacterial reduction for targeted therapy of inflammatory bowel disease, Drug Deliv. *24* (2017) 233–242, https://doi.org/10.1080/10717544.2016.1245367.
[18] A.E. Wagner, O. Will, C. Sturm, S. Lipinski, P. Rosenstiel, G. Rimbach, DSS-induced acute colitis in C57BL/6 mice is mitigated by sulforaphane pre-treatment, J. Nutr. Biochem *24* (2013) 2085–2091, https://doi.org/10.1016/j.jnutbio.2013.07.009.
[19] M. Larrosa, A. Gonzalez-Sarrias, M.J. Yanez-Gascon, M.V. Selma, M. Azorin-Ortuno, S. Toti, F. Tomas-Barberan, P. Dolara, J.C. Espin, Anti-inflammatory properties of a pomegranate extract and its metabolite urolithin-A in a colitis rat model and the effect of colon inflammation on phenolic metabolism. J. Nutr. Biochem *21* (2010) 717–725, https://doi.org/10.1016/j.jnutbio.2009.04.012.
[20] M. Larrosa, M.J. Yanez-Gascon, M.V. Selma, A. Gonzalez-Sarrias, S. Toti, J. J. Ceron, F. Tomas-Barberan, P. Dolara, J.C. Espin, Effect of a low dose of dietary resveratrol on colon microbiota, inflammation and tissue damage in a DSS-induced colitis rat model, J. Agric. Food Chem. *57* (2009) 2211–2220, https://doi.org/10.1021/jf803638d.
[21] T. Khare, S.S. Palakurthi, B.M. Shah, S. Palakurthi, S. Khare, Natural Product-Based Nanomedicine in Treatment of Inflammatory Bowel Disease, Int J. Mol. Sci. *21* (2020), https://doi.org/10.3390/ijms21113956.
[22] M.H. Farzaei, R. Rahimi, M. Abdollahi, The role of dietary polyphenols in the management of inflammatory bowel disease, Curr. Pharm. Biotechnol. *16* (2015) 196–210, https://doi.org/10.2174/1389201016666150118131704.
[23] I. Hossen, W. Hua, L. Ting, A. Mehmood, S. Jingyi, X. Duoxia, C. Yanping, W. Hongqing, G. Zhipeng, Z. Kaiqi, et al., Phytochemicals and inflammatory bowel disease: a review, Crit. Rev. Food Sci. Nutr. *60* (2020) 1321–1345, https://doi.org/10.1080/10408398.2019.1570913.
[24] C. Stanly, M. Alfieri, A. Ambrosone, A. Leone, I. Fiume, G. Pocsfalvi, Grapefruit-Derived Micro and Nanovesicles Show Distinct Metabolome Profiles and Anticancer Activities in the A375 Human Melanoma Cell Line, Cells *9* (2020), https://doi.org/10.3390/cells9122722.
[25] S. Raimondo, F. Naselli, S. Fontana, F. Monteleone, A. Lo Dico, L. Saieva, G. Zito, A. Flugy, M. Manno, M.A. Di Bella, et al., Citrus limon-derived nanovesicles inhibit cancer cell proliferation and suppress CML xenograft growth by inducing TRAIL-mediated cell death, Oncotarget *6* (2015) 19514–19527, https://doi.org/10.18632/oncotarget.4004.
[26] K. Kim, H.J. Yoo, J.H. Jung, R. Lee, J.K. Hyun, J.H. Park, D. Na, J.H. Yeon, Cytotoxic Effects of Plant Sap-Derived Extracellular Vesicles on Various Tumor Cell Types, J. Funct. Biomater. *11* (2020), https://doi.org/10.3390/jfb11020022.
[27] F. Perut, L. Roncuzzi, S. Avnet, A. Massa, N. Zini, S. Sabbadini, F. Giampieri, B. Mezzetti, N. Baldini, Strawberry-Derived Exosome-Like Nanoparticles Prevent Oxidative Stress in Human Mesenchymal Stromal Cells, Biomolecules *11* (2021), https://doi.org/10.3390/biom11010087.
[28] O. Urzi, M. Cafora, N.R. Ganji, V. Tinnirello, R. Gasparro, S. Raccosta, M. Manno, A.M. Corsale, A. Conigliaro, A. Pistocchi, et al., Lemon-derived nanovesicles achieve antioxidant and anti-inflammatory effects activating the AhR/Nrf2 signaling pathway, iScience *26* (2023) 107041, https://doi.org/10.1016/j.isci.2023.107041.
[29] Y. Teng, Y. Ren, M. Sayed, X. Hu, C. Lei, A. Kumar, E. Hutchins, J. Mu, Z. Deng, C. Luo, et al., Plant-Derived Exosomal MicroRNAs Shape the Gut Microbiota, e638, Cell Host Microbe *24* (2018) 637–652, https://doi.org/10.1016/j.chom.2018.10.001.
[30] Y. Liu, M.L. Tan, W.J. Zhu, Y.N. Cao, L.X. Peng, Z.Y. Yan, G. Zhao, In Vitro Effects of Tartary Buckwheat-Derived Nanovesicles on Gut Microbiota, J. Agric. Food Chem. *70* (2022) 2616–2629, https://doi.org/10.1021/acs.jafc.1c07658.
[31] M.Q. Lian, W.H. Chng, J. Liang, H.Q. Yeo, C.K. Lee, M. Belaid, M. Tollemeto, M. G. Wacker, B. Czarny, G. Pastorin, Plant-derived extracellular vesicles: Recent advancements and current challenges on their use for biomedical applications, J. Extra Vesicles *11* (2022) e12283, https://doi.org/10.1002/jev2.12283.
[32] O. Urzi, S. Raimondo, R. Alessandro, Extracellular Vesicles from Plants: Current Knowledge and Open Questions, Int J. Mol. Sci. *22* (2021), https://doi.org/10.3390/ijms22105366.
[33] M. Cong, S. Tan, S. Li, L. Gao, L. Huang, H.G. Zhang, H. Qiao, Technology insight: Plant-derived vesicles-How far from the clinical biotherapeutics and therapeutic drug carriers? Adv. Drug Deliv. Rev. *182* (2022) 114108 https://doi.org/10.1016/j.addr.2021.114108.
[34] V. Tinnirello, N. Rabienezhad Ganji, C. De Marcos Lousa, R. Alessandro, S. Raimondo, Exploiting the Opportunity to Use Plant-Derived Nanoparticles as Delivery Vehicles, Plants (Basel) *12* (2023), https://doi.org/10.3390/plants12061207.
[35] X. Zhuang, Z.B. Deng, J. Mu, L. Zhang, J. Yan, D. Miller, W. Feng, C.J. McClain, H. G. Zhang, Ginger-derived nanoparticles protect against alcohol-induced liver damage, J. Extra Vesicles *4* (2015) 28713, https://doi.org/10.3402/jev.v4.28713.
[36] M. Zhang, E. Viennois, M. Prasad, Y. Zhang, L. Wang, Z. Zhang, M.K. Han, B. Xiao, C. Xu, S. Srinivasan, D. Merlin, Edible ginger-derived nanoparticles: A novel therapeutic approach for the prevention and treatment of inflammatory bowel disease and colitis-associated cancer, Biomaterials *101* (2016) 321–340, https://doi.org/10.1016/j.biomaterials.2016.06.018.
[37] B. Wang, X. Zhuang, Z.B. Deng, H. Jiang, J. Mu, Q. Wang, X. Xiang, H. Guo, L. Zhang, G. Dryden, et al., Targeted drug delivery to intestinal macrophages by bioactive nanovesicles released from grapefruit, Mol. Ther. *22* (2014) 522–534, https://doi.org/10.1038/mt.2013.190.
[38] S. Ju, J. Mu, T. Dokland, X. Zhuang, Q. Wang, H. Jiang, X. Xiang, Z.B. Deng, B. Wang, L. Zhang, et al., Grape exosome-like nanoparticles induce intestinal stem cells and protect mice from DSS-induced colitis, Mol. Ther. *21* (2013) 1345–1357, https://doi.org/10.1038/mt.2013.64.
[39] M. De Robertis, A. Sarra, V. D'Oria, F. Mura, F. Bordi, P. Postorino, D. Fratantonio, Blueberry-Derived Exosome-Like Nanoparticles Counter the Response to TNF-alpha-Induced Change on Gene Expression in EA.hy926 Cells, Biomolecules *10* (2020), https://doi.org/10.3390/biom10050742.
[40] Z. Deng, Y. Rong, Y. Teng, J. Mu, X. Zhuang, M. Tseng, A. Samykutty, L. Zhang, J. Yan, D. Miller, et al., Broccoli-Derived Nanoparticle Inhibits Mouse Colitis by Activating Dendritic Cell AMP-Activated Protein Kinase, Mol. Ther. *25* (2017) 1641–1654, https://doi.org/10.1016/j.ymthe.2017.01.025.
[41] S. Raimondo, O. Urzi, S. Meraviglia, M. Di Simone, A.M. Corsale, N. Rabienezhad Ganji, A. Palumbo Piccionello, G. Polito, E. Lo Presti, F. Dieli, et al., Anti-inflammatory properties of lemon-derived extracellular vesicles are achieved through the inhibition of ERK/NF-kappaB signalling pathways, J. Cell Mol. Med *26* (2022) 4195–4209, https://doi.org/10.1111/jcmm.17404.
[42] N. Rabienezhad Ganji, O. Urzi, V. Tinnirello, E. Costanzo, G. Polito, A. Palumbo Piccionello, M. Manno, S. Raccosta, A. Gallo, M. Lo Pinto, et al., Proof-of-Concept Study on the Use of Tangerine-Derived Nanovesicles as siRNA Delivery Vehicles toward Colorectal Cancer Cell Line SW480, Int J. Mol. Sci. *25* (2023), https://doi.org/10.3390/ijms25010546.
[43] H. Shiratori, C. Feinweber, S. Luckhardt, B. Linke, E. Resch, G. Geisslinger, A. Weigert, M.J. Parnham, THP-1 and human peripheral blood mononuclear cell-derived macrophages differ in their capacity to polarize in vitro, Mol. Immunol. *88* (2017) 58–68, https://doi.org/10.1016/j.molimm.2017.05.027.
[44] M. Pucci, S. Raimondo, O. Urzi, M. Moschetti, M.A. Di Bella, A. Conigliaro, N. Caccamo, M.P. La Manna, S. Fontana, R. Alessandro, Tumor-Derived Small Extracellular Vesicles Induce Pro-Inflammatory Cytokine Expression and PD-L1 Regulation in M0 Macrophages via IL-6/STAT3 and TLR4 Signaling Pathways, Int J. Mol. Sci. *22* (2021), https://doi.org/10.3390/ijms222212118.
[45] M.G. Zizzo, G. Caldara, A. Bellanca, D. Nuzzo, M. Di Carlo, S. Scoglio, R. Serio, AphaMax((R)), an Aphanizomenon Flos-Aquae Aqueous Extract, Exerts Intestinal Protective Effects in Experimental Colitis in Rats. Nutrients *12* (2020) https://doi.org/10.3390/nu12123635.
[46] F. Kullmann, H. Messmann, M. Alt, V. Gross, T. Bocker, J. Scholmerich, J. Ruschoff, Clinical and histopathological features of dextran sulfate sodium induced acute and chronic colitis associated with dysplasia in rats, Int J. Colorectal Dis. *16* (2001) 238–246, https://doi.org/10.1007/s003840100311.
[47] C.B. Appleyard, J.L. Wallace, Reactivation of hapten-induced colitis and its prevention by anti-inflammatory drugs, Am. J. Physiol. *269* (1995) G119–G125, https://doi.org/10.1152/ajpgi.1995.269.1.G119.
[48] T.G. Moreels, R.J. Nieuwendijk, J.G. De Man, B.Y. De Winter, A.G. Herman, E. A. Van Marck, P.A. Pelckmans, Concurrent infection with Schistosoma mansoni attenuates inflammation induced changes in colonic morphology, cytokine levels, and smooth muscle contractility of trinitrobenzene sulphonic acid induced colitis in rats, Gut *53* (2004) 99–107, https://doi.org/10.1136/gut.53.1.99.
[49] G. Guggino, D. Mauro, A. Rizzo, R. Alessandro, S. Raimondo, A.S. Bergot, M. A. Rahman, J.J. Ellis, S. Milling, R. Lories, et al., Inflammasome Activation in Ankylosing Spondylitis Is Associated With Gut Dysbiosis, Arthritis Rheuma *73* (2021) 1189–1199, https://doi.org/10.1002/art.41644.
[50] E. Bolyen, J.R. Rideout, M.R. Dillon, N.A. Bokulich, C.C. Abnet, G.A. Al-Ghalith, H. Alexander, E.J. Alm, M. Arumugam, F. Asnicar, et al., Reproducible, interactive, scalable and extensible microbiome data science using QIIME 2, Nat. Biotechnol. *37* (2019) 852–857, https://doi.org/10.1038/s41587-019-0209-9.
[51] B.J. Callahan, P.J. McMurdie, M.J. Rosen, A.W. Han, A.J. Johnson, S.P. Holmes, DADA2: High-resolution sample inference from Illumina amplicon data, Nat. Methods *13* (2016) 581–583, https://doi.org/10.1038/nmeth.3869.
52 F. Pedregosa, G. Varoquaux, A. Gramfort, V. Michel, B. Thirion, O. Grisel, M. Blondel, P. Prettenhofer, R. Weiss, V. Dubourg, et al., Scikit-learn: Machine Learning, Python. J. Mach. Learn. Res. *12* (2011) 2825–2830.
[53] B.D. Kaehler, N.A. Bokulich, D. McDonald, R. Knight, J.G. Caporaso, G.A. Huttley, Species abundance information improves sequence taxonomy classification accuracy, Nat. Commun. *10* (2019) 4643, https://doi.org/10.1038/s41467-019-12669-6.
[54] Y. Benjamini, Y. Hochberg, Controlling the False Discovery Rate - a Practical and Powerful Approach to Multiple Testing, J. R. Stat. Soc. B *57* (1995) 289–300, https://doi.org/10.1111/j.2517-6161.1995.tb02031.x.
[55] C. Zhao, F. Wang, Y. Lian, H. Xiao, J. Zheng, Biosynthesis of citrus flavonoids and their health effects, Crit. Rev. Food Sci. Nutr. *60* (2020) 566–583, https://doi.org/10.1080/10408398.2018.1544885.
[56] F. Alam, K. Mohammadin, Z. Shafique, S.T. Amjad, M. Asad, Citrus flavonoids as potential therapeutic agents: A review, Phytother. Res *36* (2022) 1417–1441, https://doi.org/10.1002/ptr.7261.
[57] V. Morampudi, G. Bhinder, X. Wu, C. Dai, H.P. Sham, B.A. Vallance, K. Jacobson, DNBS/TNBS colitis models: providing insights into inflammatory bowel disease and effects of dietary fat, J. Vis. Exp. (2014) e51297, https://doi.org/10.3791/51297.
[58] V. Villanacci, R. Del Sordo, T.L. Parigi, G. Leoncini, G. Bassotti, Inflammatory Bowel Diseases: Does One Histological Score Fit All? Diagn. (Basel) *13* (2023) https://doi.org/10.3390/diagnostics13122112.

[59] E.A. Sankey, A.P. Dhillon, A. Anthony, A.J. Wakefield, R. Sim, L. More, M. Hudson, A.M. Sawyerr, R.E. Pounder, Early mucosal changes in Crohn's disease, Gut *34* (1993) 375–381, https://doi.org/10.1136/gut.34.3.375.

[60] R.K. Yantiss, R.D. Odze, Diagnostic difficulties in inflammatory bowel disease pathology, Histopathology *48* (2006) 116–132, https://doi.org/10.1111/j.1365-2559.2005.02248.x.

[61] J.J. Kim, M.S. Shajib, M.M. Manocha, W.I. Khan, Investigating intestinal inflammation in DSS-induced model of IBD, J. Vis. Exp. (2012), https://doi.org/10.3791/3678.

[62] G. Ndrepepa, Myeloperoxidase - A bridge linking inflammation and oxidative stress with cardiovascular disease, Clin. Chim. Acta *493* (2019) 36–51, https://doi.org/10.1016/j.cca.2019.02.022.

[63] W.T. Kuo, L. Zuo, M.A. Odenwald, S. Madha, G. Singh, C.B. Gurniak, C. Abraham, J.R. Turner, The Tight Junction Protein ZO-1 Is Dispensable for Barrier Function but Critical for Effective Mucosal Repair, Gastroenterology *161* (2021) 1924–1939, https://doi.org/10.1053/j.gastro.2021.08.047.

[64] D. Hollander, C.M. Vadheim, E. Brettholz, G.M. Petersen, T. Delahunty, J. I. Rotter, Increased intestinal permeability in patients with Crohn's disease and their relatives. A possible etiologic factor, Ann. Intern Med *105* (1986) 883–885, https://doi.org/10.7326/0003-4819-105-6-883.

[65] W.T. Kuo, L. Shen, L. Zuo, N. Shashikanth, M. Ong, L. Wu, J. Zha, K.L. Edelblum, Y. Wang, S.P. Nilsen, J.R. Turner, Inflammation-induced Occludin Downregulation Limits Epithelial Apoptosis by Suppressing Caspase-3 Expression, Gastroenterology *157* (2019) 1323–1337, https://doi.org/10.1053/j.gastro.2019.07.058.

[66] N. Chhikara, R. Kour, S. Jaglan, P. Gupta, Y. Gat, A. Panghal, Citrus medica: nutritional, phytochemical composition and health benefits - a review, Food Funct. *9* (2018) 1978–1992, https://doi.org/10.1039/c7fo02035j.

[67] X. Lu, C. Zhao, H. Shi, Y. Liao, F. Xu, H. Du, H. Xiao, J. Zheng, Nutrients and bioactives in citrus fruits: Different citrus varieties, fruit parts, and growth stages, Crit. Rev. Food Sci. Nutr. *63* (2023) 2018–2041, https://doi.org/10.1080/10408398.2021.1969891.

[68] Y. Wang, X.J. Liu, J.B. Chen, J.P. Cao, X. Li, C.D. Sun, Citrus flavonoids and their antioxidant evaluation, Crit. Rev. Food Sci. Nutr. *62* (2022) 3833–3854, https://doi.org/10.1080/10408398.2020.1870035.

[69] G.C. Rampersaud, M.F. Valim, 100% citrus juice: Nutritional contribution, dietary benefits, and association with anthropometric measures, Crit. Rev. Food Sci. Nutr. *57* (2017) 129–140, https://doi.org/10.1080/10408398.2013.862611.

[70] Z. Zou, W. Xi, Y. Hu, C. Nie, Z. Zhou, Antioxidant activity of Citrus fruits, Food Chem. *196* (2016) 885–896, https://doi.org/10.1016/j.foodchem.2015.09.072.

[71] M. Coimbra, B. Isacchi, L. van Bloois, J.S. Torano, A. Ket, X. Wu, F. Broere, J. M. Metselaar, C.J. Rijcken, G. Storm, et al., Improving solubility and chemical stability of natural compounds for medicinal use by incorporation into liposomes, Int J. Pharm. *416* (2011) 433–442, https://doi.org/10.1016/j.ijpharm.2011.01.056.

[72] A. Ali, C.H. Chong, S.H. Mah, L.C. Abdullah, T.S.Y. Choong, B.L. Chua, Impact of Storage Conditions on the Stability of Predominant Phenolic Constituents and Antioxidant Activity of Dried Piper betle Extracts, Molecules *23* (2018), https://doi.org/10.3390/molecules23020484.

[73] J.D. Lewis, R.S. Sandler, C. Brotherton, C. Brensinger, H. Li, M.D. Kappelman, S. G. Daniel, K. Bittinger, L. Albenberg, J.F. Valentine, et al., A Randomized Trial Comparing the Specific Carbohydrate Diet to a Mediterranean Diet in Adults With Crohn's Disease, e839, Gastroenterology *161* (2021) 837–852, https://doi.org/10.1053/j.gastro.2021.05.047.

[74] F. Chicco, S. Magri, A. Cingolani, D. Paduano, M. Pesenti, F. Zara, F. Tumbarello, E. Urru, A. Melis, L. Casula, et al., Multidimensional Impact of Mediterranean Diet on IBD Patients, Inflamm. Bowel Dis. *27* (2021) 1–9, https://doi.org/10.1093/ibd/izaa097.

[75] M. Chagas, M.D. Behrens, C.J. Moragas-Tellis, G.X.M. Penedo, A.R. Silva, C. F. Goncalves-de-Albuquerque, Flavonols and Flavones as Potential anti-Inflammatory, Antioxidant, and Antibacterial Compounds, Oxid. Med Cell Longev. *2022* (2022) 9966750, https://doi.org/10.1155/2022/9966750.

[76] S.J. Maleki, J.F. Crespo, B. Cabanillas, Anti-inflammatory effects of flavonoids, Food Chem. *299* (2019) 125124, https://doi.org/10.1016/j.foodchem.2019.125124.

[77] J.H. Hwang, Y.S. Park, H.S. Kim, D.H. Kim, S.H. Lee, C.H. Lee, J.E. Kim, S. Lee, H. M. Kim, H.W. Kim, et al., Yam-derived exosome-like nanovesicles stimulate osteoblast formation and prevent osteoporosis in mice, J. Control Release *355* (2023) 184–198, https://doi.org/10.1016/j.jconrel.2023.01.071.

[78] J. Cai, J. Pan, Beta vulgaris-derived exosome-like nanovesicles alleviate chronic doxorubicin-induced cardiotoxicity by inhibiting ferroptosis, J. Biochem Mol. Toxicol. (2023) e23540, https://doi.org/10.1002/jbt.23540.

[79] E. Berger, P. Colosetti, A. Jalabert, E. Meugnier, O.P.B. Wiklander, J. Jouhet, E. Errazurig-Cerda, S. Chanon, D. Gupta, G.J.P. Rautureau, et al., Use of Nanovesicles from Orange Juice to Reverse Diet-Induced Gut Modifications in Diet-Induced Obese Mice, Mol. Ther. Methods Clin. Dev. *18* (2020) 880–892, https://doi.org/10.1016/j.omtm.2020.08.009.

[80] C. Gao, Y. Zhou, Z. Chen, H. Li, Y. Xiao, W. Hao, Y. Zhu, C.T. Vong, M.A. Farag, Y. Wang, S. Wang, Turmeric-derived nanovesicles as novel nanobiologics for targeted therapy of ulcerative colitis, Theranostics *12* (2022) 5596–5614, https://doi.org/10.7150/thno.73650.

[81] Z. Zhu, L. Liao, M. Gao, Q. Liu, Garlic-derived exosome-like nanovesicles alleviate dextran sulphate sodium-induced mouse colitis via the TLR4/MyD88/NF-kappaB pathway and gut microbiota modulation. Food Funct. *14* (2023) 7520–7534, https://doi.org/10.1039/d3fo01094e.

[82] A. Salminen, M. Lehtonen, T. Suuronen, K. Kaarniranta, J. Huuskonen, Terpenoids: natural inhibitors of NF-kappaB signaling with anti-inflammatory and anticancer potential. Cell Mol. Life Sci. *65* (2008) 2979–2999, https://doi.org/10.1007/s00018-008-8103-5.

[83] T. Lawrence, The nuclear factor NF-kappaB pathway in inflammation, Cold Spring Harb. Perspect. Biol. *1* (2009) a001651, https://doi.org/10.1101/cshperspect.a001651.

[84] T. Liu, L. Zhang, D. Joo, S.C. Sun, NF-kappaB signaling in inflammation., 17023-, Signal Transduct. Target Ther. *2* (2017), https://doi.org/10.1038/sigtrans.2017.23.

[85] J. Landy, E. Ronde, N. English, S.K. Clark, A.L. Hart, S.C. Knight, P.J. Ciclitira, H. O. Al-Hassi, Tight junctions in inflammatory bowel diseases and inflammatory bowel disease associated colorectal cancer, World J. Gastroenterol. *22* (2016) 3117–3126, https://doi.org/10.3748/wjg.v22.i11.3117.

[86] Z. Xiong, Y. Cui, J. Wu, L. Shi, W. Quan, S. Yang, Y. Feng, Luteolin-7-O-rutinoside from Pteris cretica L. var. nervosa attenuates LPS/D-gal-induced acute liver injury by inhibiting PI3K/AKT/AMPK/NF-kappaB signaling pathway. Naunyn Schmiede Arch. Pharm. *395* (2022) 1283–1295, https://doi.org/10.1007/s00210-022-02266-8.

[87] T. Chen, X. Zhang, G. Zhu, H. Liu, J. Chen, Y. Wang, X. He, Quercetin inhibits TNF-alpha induced HUVECs apoptosis and inflammation via downregulating NF-kB and AP-1 signaling pathway in vitro, Med. (Baltim. ) *99* (2020) e22241, https://doi.org/10.1097/MD.0000000000022241.

[88] O.J. Sul, S.W. Ra, Quercetin prevents LPS-induced oxidative stress and inflammation by modulating NOX2/ROS/NF-kB in lung epithelial cells, Molecules *26* (2021), https://doi.org/10.3390/molecules26226949.

[89] H. Parhiz, A. Roohbakhsh, F. Soltani, R. Rezaee, M. Iranshahi, Antioxidant and anti-inflammatory properties of the citrus flavonoids hesperidin and hesperetin: an updated review of their molecular mechanisms and experimental models, Phytother. Res *29* (2015) 323–331, https://doi.org/10.1002/ptr.5256.

[90] J. Li, T. Wang, P. Liu, F. Yang, X. Wang, W. Zheng, W. Sun, Hesperetin ameliorates hepatic oxidative stress and inflammation via the PI3K/AKT-Nrf2-ARE pathway in oleic acid-induced HepG2 cells and a rat model of high-fat diet-induced NAFLD, Food Funct. *12* (2021) 3898–3918, https://doi.org/10.1039/d0fo02736g.

[91] J. Xu, L. Ma, P. Fu, Eriocitrin attenuates ischemia reperfusion-induced oxidative stress and inflammation in rats with acute kidney injury by regulating the dual-specificity phosphatase 14 (DUSP14)-mediated Nrf2 and nuclear factor-kappaB (NF-kappaB) pathways, Ann. Transl. Med *9* (2021) 350, https://doi.org/10.21037/atm-21-337.

[92] G. Guo, W. Shi, F. Shi, W. Gong, F. Li, G. Zhou, J. She, Anti-inflammatory effects of eriocitrin against the dextran sulfate sodium-induced experimental colitis in murine model, J. Biochem Mol. Toxicol. *33* (2019) e22400, https://doi.org/10.1002/jbt.22400.

[93] F. Sommer, J.M. Anderson, R. Bharti, J. Raes, P. Rosenstiel, The resilience of the intestinal microbiota influences health and disease, Nat. Rev. Microbiol *15* (2017) 630–638, https://doi.org/10.1038/nrmicro.2017.58.

[94] A. Nishida, K. Nishino, K. Sakai, Y. Owaki, Y. Noda, H. Imaeda, Can control of gut microbiota be a future therapeutic option for inflammatory bowel disease? World J. Gastroenterol. *27* (2021) 3317–3326, https://doi.org/10.3748/wjg.v27.i23.3317.

[95] A. Nishida, R. Inoue, O. Inatomi, S. Bamba, Y. Naito, A. Andoh, Gut microbiota in the pathogenesis of inflammatory bowel disease, Clin. J. Gastroenterol. *11* (2018) 1–10, https://doi.org/10.1007/s12328-017-0813-5.

[96] R.H. Dahal, S. Kim, Y.K. Kim, E.S. Kim, J. Kim, Insight into gut dysbiosis of patients with inflammatory bowel disease and ischemic colitis, Front Microbiol *14* (2023) 1174832, https://doi.org/10.3389/fmicb.2023.1174832.

[97] E.J. Choi, H.J. Lee, W.J. Kim, K.I. Han, M. Iwasa, K. Kobayashi, T. Debnath, Y. Tang, Y.S. Kwak, J.H. Yoon, E.K. Kim, Enterococcus faecalis EF-2001 protects DNBS-induced inflammatory bowel disease in mice model, PLoS One *14* (2019) e0210854, https://doi.org/10.1371/journal.pone.0210854.

[98] K.K. Jang, T. Heaney, M. London, Y. Ding, G. Putzel, F. Yeung, D. Ercelen, Y. H. Chen, J. Axelrad, S. Gurunathan, et al., Antimicrobial overproduction sustains intestinal inflammation by inhibiting Enterococcus colonization, e1458, Cell Host Microbe *31* (2023) 1450–1468, https://doi.org/10.1016/j.chom.2023.08.002.

[99] G.L. D'Adamo, M. Chonwerawong, L.J. Gearing, V.R. Marcelino, J.A. Gould, E. L. Rutten, S.M. Solari, P.W.R. Khoo, T.J. Wilson, T. Thomason, et al., Bacterial clade-specific analysis identifies distinct epithelial responses in inflammatory bowel disease, Cell Rep. Med *4* (2023) 101124, https://doi.org/10.1016/j.xcrm.2023.101124.

[100] I. Masoodi, A.S. Alshanqeeti, E.J. Alyamani, A.A. AlLehibi, A.N. Alqutub, K. N. Alsayari, A.O. Alomair, Microbial dysbiosis in irritable bowel syndrome: A single-center metagenomic study in Saudi Arabia, JGH Open *4* (2020) 649–655, https://doi.org/10.1002/jgh3.12313.

[101] L.K. Brahe, E. Le Chatelier, E. Prifti, N. Pons, S. Kennedy, T. Hansen, O. Pedersen, A. Astrup, S.D. Ehrlich, L.H. Larsen, Specific gut microbiota features and metabolic markers in postmenopausal women with obesity, Nutr. Diabetes *5* (2015) e159, https://doi.org/10.1038/nutd.2015.9.

[102] S.Y. Chen, M.H. Weng, Z.Y. Li, G.Y. Wang, G.C. Yen, Protective effects of camellia and olive oils against cognitive impairment via gut microbiota-brain communication in rats, Food Funct. *13* (2022) 7168–7180, https://doi.org/10.1039/d1fo04418d.

[103] M. Vacca, G. Celano, F.M. Calabrese, P. Portincasa, M. Gobbetti, M. De Angelis, The Controversial Role of Human Gut Lachnospiraceae, Microorganisms *8* (2020), https://doi.org/10.3390/microorganisms8040573.

[104] R. Garcia-Villalba, D. Beltran, M.D. Frutos, M.V. Selma, J.C. Espin, F.A. Tomas-Barberan, Metabolism of different dietary phenolic compounds by the urolithin-producing human-gut bacteria Gordonibacter urolithinfaciens and Ellagibacter isourolithinifaciens, Food Funct. *11* (2020) 7012–7022, https://doi.org/10.1039/d0fo01649g.

[105] Y. Yan, L. Li, K. Wu, G. Zhang, L. Peng, Y. Liang, Z. Wang, A Combination of Baicalin and Berberine Hydrochloride Ameliorates Dextran Sulfate Sodium-Induced Colitis by Modulating Colon Gut Microbiota, J. Med Food *25* (2022) 853–862, https://doi.org/10.1089/jmf.2021.K.0173.

[106] C. Alexander, M. Brauchla, K.D. Sanoshy, T.M. Blonquist, G.N. Maloney, E. Mah, K. Kelley-Garvin, O. Chen, D.J. Liska, J.E. Shin, et al., Bowel habits, faecal microbiota and faecal bile acid composition of healthy adults consuming fruit pomace fibres: two-arm, randomised, double-blinded, placebo-controlled trials, Br. J. Nutr. *130* (2023) 42–55, https://doi.org/10.1017/S0007114522002951.

[107] C. Lee, S.N. Hong, N.Y. Paik, T.J. Kim, E.R. Kim, D.K. Chang, Y.H. Kim, CD1d modulates colonic inflammation in NOD2-/- mice by altering the intestinal microbial composition comprising acetatifactor muris, J. Crohns Colitis *13* (2019) 1081–1091, https://doi.org/10.1093/ecco-jcc/jjz025.

[108] G. den Besten, K. van Eunen, A.K. Groen, K. Venema, D.J. Reijngoud, B.M. Bakker, The role of short-chain fatty acids in the interplay between diet, gut microbiota, and host energy metabolism, J. Lipid Res *54* (2013) 2325–2340, https://doi.org/10.1194/jlr.R036012.

[109] C. Manichanh, N. Borruel, F. Casellas, F. Guarner, The gut microbiota in IBD, Nat. Rev. Gastroenterol. Hepatol. *9* (2012) 599–608, https://doi.org/10.1038/nrgastro.2012.152.